UNIVERSITY OF CALIFORNIA, SAN DIEGO

Study of Sestrin in Eye Growth Regulation, Lipid Physiology, Heart Function and Domain Study of *dSesn* and *mSesn1*

A thesis submitted in partial satisfaction of the requirements for the degree
Master of Science

in

Biology

by

Teddy Earl Kim

Committee in charge:

Professor Ethan Bier, Chair
Professor Jon Chris Armour
Professor James Wilhelm

2010

ProQuest LLC
789 East Eisenhower Parkway
P.O. Box 1346
Ann Arbor, MI 48106-1346

The thesis of Teddy Earl Kim is approved, and it is acceptable in quality and form for publication in microfilm and electronically:

_____

_____

_____

Chair

University of California, San Diego

2010

Dedication

I would like to dedicate my Master of Science thesis to my mother, who has always supported me with my young academic career, my sister, who I care for the most in this entire world, Lollie, who brought new joy to our family, and to my father, who taught me how to be a man and is still the reason why I strive each and everyday.

Epigraph

"I firmly believe that any man's finest hour – his greatest fulfillment to all he holds dear – is that moment when he has worked his heart out in a good cause and lies exhausted on the field of battle – victorious"

-Vince Lombardi

Table of Contents

List of Figures

Acknowledgments

I would like to thank and acknowledge Dr. Jun Hee Lee for teaching me the biochemical and genetic techniques necessary to perform my Master work.

I would also like to thank Dr. Andrei Budanov for the continual assistance and consultation throughout the project.

I would also like to acknowledge Dr. Eek Joong Park for the assistance throughout the project and also for being a great mentor.

I would like to thank Dr. Ryan Birse for teaching me the heart recording techniques necessary to perform cardiac function measurements in figure 4 and figure 5.

I would like to thank Dr. Guy Perkins for producing the electron microscope images that I was able to use to produce my data in figure 2.

I would also like to thank Dr. Karen Ocorr for assisting and teaching the fly heart recording technique that I was able to use for my studies in figure 4 and figure 5.

I would like to thank Dr. Mark Ellisman for producing the electron microscope images in figure 2.

I would like to thank Dr. Rolf Bodmer for allowing me to use his lab for the heart recording experiments.

I would like to thank Dr. Ethan Bier for allowing me to use his lab to perform *Drosophila* genetic studies and also being a mentor for me throughout my studies.

Lastly, I would like to thank Dr. Michael Karin for being a wonderful advisor and mentor throughout my studies.

ABSTRACT OF THE THESIS

Study of Sestrin in Eye Growth Regulation, Lipid Physiology, Heart Function and Domain Study of *dSesn* and *mSesn1*

by

Teddy Earl Kim

Master of Science in Biology

University of California, San Diego, 2010

Professor Ethan Bier, Chair

Sestrin is a family of proteins known to regulate cell growth by TOR signaling modulation. While Overexpression of *dSesn* in the eye only caused a slight reduction in size, coexpression of *dSesn* with TOR activators caused a reduction in size compared to single expression of TOR activators in the eye. Immunoblots indicate that TOR signaling is reduced with the expression of *dSesn*, indicated by reduced phosphorylation of TOR targets, 4E-BP and S6K. The $dSesn^{-/-}$ organisms showed increased lipid accumulation compared to wildtype, which was suppressed by AICAR and rapamycin feeding or expression of wildtype *dSesn.* Immunoblots of larvae fat bodies indicate that $dSesn^{-/-}$ organisms have decreased AMPK phosphorylation and increased S6K and 4E-BP phosphorylation. Cardiac function of $dSesn^{-/-}$ organism shows reduced heart rate, increased arrhythmia and increased diameter, which were rescued by rapamycin and AICAR feeding. Administration of vitamin E, an antioxidant, only rescued arrhythmia. *Hand-GAL4* driver was used to express TOR downstream components specifically at the heart. Overexpression of an active form of 4E-BP suppressed translation to decrease heart

diameter and rescue *dSesn*$^{-/-}$ heart rate, while overexpression of *Atg1* resulted in aggravating arrhythmicity. NOVA screening of *dSesn* and *mSesn1* may provide insights into understanding the structural basis of Sestrins. NOVA screening on 50,000 (*dSesn*) and 35,000 (*mSesn1*) flies in eyes and wings was performed, however, failed to isolate novel mutations that affect Sestrin function. Alternative genetic strategies, such as suppression of synthetic lethality by strong expression of Sestrins, may be used to improve sensitivity of the NOVA screening.

Introduction

Cell growth is an extensively coordinated process that is regulated in both time and space (Wullscheleger et al., 2004). It has been well documented that the target of rapamycin (TOR) is a key regulator of cell growth and is well conserved in all eukaryotes (Wullscheleger et al., 2004, Oldham et al., 2002, Hay et al., 2004, Martin et al., 2005, and Grewal et al., 2009). Rapamycin was originally isolated from a soil sample from Rapa Nui and is known to inhibit TOR signaling by binding to the FRB domain by making a complex with a cofactor FKBP12 (Wullscheleger et al., 2004, Oldham et al., 2002, and Martin et al., 2005). Since cell growth is an extensively energy consuming process, regulation of cell growth is essential for the proper growth of the organism by promoting cell growth only under favorable conditions. Growth arrest phenotypes and systemic defects observed in TOR mutant organisms in metazoans strongly suggest that metazoan TOR coordinates growth and development in response to nutritional cues (Wullscheleger et al., 2004). When growth conditions are favorable, active TOR allows cells to maintain a robust rate of ribosome biogenesis, translation initiation, and nutrient import (Wullscheleger et al., 2004). However, downregulation of TOR activity by the treatment with rapamycin, starved for nitrogen, or genetic mutation of TOR dramatically downregulate general protein synthesis, upregulate macroautophagy and activate several stress-responsive transcription factors (Wullscheleger et al., 2004), which indicate the important role TOR signaling cascade plays in growth regulation. TOR activity is modulated by multiple upstream regulators and exerts its effect by modulating the activity of multiple downstream effector proteins that alter different cellular functions (Wullscheleger et al., 2004).

Further purification of TOR1 and TOR2 from yeasts led to the understanding that there are two TOR complexes, TORC1 and TORC2, of which only TORC1 is responsive to rapamycin-FKBP12 inhibition (Wullscheleger et al., 2004, and Oldham et al., 2002). It was suggested that TORC1 is responsible for temporal growth control and TORC2 is responsible for spatial growth control (Wullscheleger et al., 2004 and Martin et al., 2005). The two different TOR complexes consist of different subunits that are well conserved from yeast to mammals (Wullscheleger et al., 2004, Oldham et al., 2002, Hay et al., 2004, Martin et al., 2005, and Grewal et al., 2009). Mammalian TORC1 (mTORC1) is composed of mammalian LST8 (mLST8) and Raptor while mammalian TORC2 (mTORC2) is composed of mLST8 and Rictor (Wullscheleger et al., 2004). Rapamycin-FKBP12 inhibition takes place when the complex binds to mTORC1 just to the amino end of the kinase domain (Wullscheleger et al., 2004). While each component of the TOR complex is crucial for the functionality of TOR kinase activity, the function of individual components on mTORC1 is poorly understood. For instance, different labs suggest that Raptor functions as an adaptor molecule to recruit the different components of mTORC1 while others suggest that Raptor-mTOR interaction is modulated by upstream signals to regulate mTORC1 signaling (Wullscheleger et al., 2004). In either case, knockdown experiments using RNAi system in mammalian cells indicate that Raptor is essential for TOR functionality (Hay et al., 2004). The exact mechanism by which rapamycin-FKBP12 inhibits mTORC1 is not fully understood (Wullscheleger et al., 2004). Different suggestions have been made from rapamycin-FKBP12 inhibiting the kinase domain to rapamycin-FKBP12 causing mTORC1 complex dissociation (Wullscheleger et al., 2004). mLST8, a component involved in both mTORC1 and mTORC2 is also found to have

positive effects on TOR signaling, however, the exact function is yet unknown (Wullscheleger et al., 2004).

TOR is a key regulator of cell growth and metabolism in response to environmental cues and availability of nutrients (Wullscheleger et al., 2004, Oldham et al., 2002, Hay et al., 2004, and Martin et al., 2005). As depicted in Figure 1, the major activating signal of TOR is via the insulin receptor (InR) and its downstream components operated by phosphoinositide 3-kinase (PI3K) to recruit phosphoinositide dependent kinase 1 (PDK1) and Akt (also called PKB) (Oldham et al., 2002, Hay et al., 2004, and Martin et al., 2005). The activity of PI3K is inhibited by a lipid phosphatase, phosphatase and tensin homolog (PTEN), resulting in down regulation of TOR signaling (Oldham et al., 2002). The activation of protein kinase Akt by PDK1 results in the phosphorylation of tuberous sclerosis protein 2 (TSC2) (Wullscheleger et al., 2004, and Hay et al., 2004). TSC2 (tuberin) acts as a heterodimer with TSC1 (hamartin) and becomes functionally inactivated, preventing heterodimer formation when phosphorylated by Akt (Wullscheleger et al., 2004, and Martin et al., 2005). The negative growth regulating effect of TSC1/2 heterodimer was observed when TSC1 and TSC2 were overexpressed together, but not when only one component was overexpressed alone (Hay et al., 2004). When TSC1/2 heterodimer forms, TSC2 acts as a GTPase activating protein (GAP) to activate Rheb, a small GTPase (Wullscheleger et al., 2004, Oldham et al., 2002, Hay et al., 2004). Rheb is able to bind to TOR in a GTP dependent manner to cause TOR activation (Wullscheleger et al., 2004). However, the binding of Rheb onto TOR is not nucleotide dependent and can cause TOR inactivation in the absence of GTP (Wullscheleger et al., 2004, and Oldham et al., 2002). TOR, when activated, acts as a

serine/theronine kinase that phosphorylates its downstream effectors to modulate cell growth (Oldham et al., 2002). Activated TOR causes multiple down stream signal activation by phosphorylating different components involved in processes such as cell growth regulation, transcription, translation, and autophagy (Wullscheleger et al., 2004).

TOR activation first promotes cell growth by phosphorylating p70 S6K, which phosphorylates 40S ribosomal protein S6 to promote translation of mRNAs containing 5' tract of oligopyrimidine (TOP) (Wullscheleger et al., 2004, Oldham et al., 2002, Hay et al., 2004, and Martin et al., 2005). In addition, TOR also phosphorylates eukaryotic initiation factor 4E (eIF4E)-binding protein (4E-BP), which causes dissociation of eIF4E to stimulate translation by binding to eIF4G (Wullscheleger et al., 2004, and Hay et al., 2004). TOR activation also plays a crucial role in controlling macroauthophagy, which is a cellular compensatory mechanism to adapt to stress and starvation (Wullscheleger et al., 2004). TOR phosphorylates Atg1 and Atg13, which prevent the activation of autophagy-associated components from forming an Atg1/Atg13/Atg17 complex that induce autophagy (Chan, 2009). The details regarding the autophagy activation event still requires further investigation as there are multiple phosphorylation sites in Atg1 protein that is also found to go through autophosphorylation (Chan, 2009). Recently, Akt mediated sterol regulatory element binding proteins (SREBP) is a transcription factor that has been found to be activated by TOR and control organ growth (Porstmann et al., 2008). SREBP is synthesized as inactive presursors and localize to the ER, where they bind to sterol cleavage activating protein (SCAP) (Porstmann et al., 2008). SREBP/SCAP complex is further processed by cleaving the N-terminal half of the SREBP, which allows the molecule to localize in the nucleus and bind to sterol regulatory element and E box

sequences found in promoter regions of genes involved in cholesterol and fatty acid biosynthesis (Porstmann et al., 2008). Akt activation is shown to have an upregulation of ATP-citrate lyase (ACLY) and fatty acid synthase (FASN), which are reguired to divert glycolytic carbon flux into lipid biosynthesis (Porstmann et al., 2008). It was shown that the Akt mediated increase in cell growth required the induction of lipid biosynthesis as the inhibition of ACLY abolished Akt mediated increase in cell volume (Porstmann et al., 2008). Upon Akt activation, nuclear mature SREBP (mSREBP) was detected within 2 hours of Akt activation and a subsequent increase in FASN mRNA levels within 4 hours of Akt induction (Porstmann et al., 2008). Further experimental results suggest that the silencing of mTOR or Raptor, but not Rictor, abolishes the induction of lipogenesis in response to Akt activation (Porstmann et al., 2008). When tested in the *Drosophila*, the ablation of dSREBP expression using RNAi in an organ specific manner showed reduction in tissue size while maintaining the same number of cells (Porstmann et al., 2008). Therefore, these results suggest that SREBP is another downstream target of TOR signaling, which is responsible for cell growth regulation as well as *de novo* lipogenesis.

The fact that TOR signaling is regulated upon energy and nutrient availability indicates that cell growth regulation is crucial for cell survival since mRNA translation and ribosomal biogenesis are processes that require high levels of energy (Hay et al., 2004). The TOR signaling senses energy availability through the 5'AMP-activated protein kinase (AMPK) (Wullscheleger et al., 2004, Hay et al., 2004, and Martin et al., 2005). AMPK is modulated by even moderate changes in the AMP/ATP ratio can reduce TOR signaling when activated by 5-aminoomidazole-4-carboxyamide (AICAR) indicated by altered S6K phosphorylation levels (Hay et al., 2004, and Martin et al., 2005). AICAR

is a pharmacological activator of AMPK. AICAR is transported into cells via adenosine receptors and forms an AMP homolog ZMP, which results in increased AMP/ATP ratio to cause AMPK activation (Towler et al., 2006). This process is also mTOR dependent since the S6K variant that is not sensitive to rapamycin is not affected upon AMPK activation via AICAR (Hay et al., 2004). This link provides an important level of control for energy-availability-dependent-cell-growth and suggests that energy, metabolism and protein synthesis are closely coupled (Hay et al., 2004). TOR signaling is also shown to have increased activity upon amino acid availability (Wullscheleger et al., 2004, Oldham et al., 2002, Hay et al., 2004, and Martin et al., 2005). Such findings make sense in an evolutionary perspective since it would be disadvantageous to promote cell growth under nutrient poor conditions. Promoting cell growth only under favorable conditions would enhance the organisms' ability to survive by conserving energy in situations when there is low nutrient availability. However, the exact mechanisms is not yet known if amino acids are sensed at the level of TOR, Rheb or the TSC1/2 complex (Martin et al., 2005).

A member of the Sestrin family of genes was originally identified as p53-dependent genes induced in response to genotoxic damage such as UV radiation, γ-radiation or the treatment with an anticancer drug doxorubicin and was called *PA26* (p53 activated gene #26) (Velasco-Miguel et al., 1999). After this finding, a different group identified a gene shown to have delayed activation in response to hypoxic conditions and was named *Hi95* (hypoxia induced gene #95), which also showed close homology to the previously described gene *PA26* (Budanov et al., 2002). Later, *PA26* and *Hi95* were renamed *mammalian Sestrin 1* (*mSesn1*) and *mammalian Sestrin 2* (*mSesn2*) respectively. It is interesting to note that while *PA26/mSesn1* show p53 dependent induction under

hypoxia and DNA damage, *Hi95/mSesn2* show p53 dependent induction under DNA damage but p53 independent induction under hypoxia (Budanov et al., 2002). Sestrin genes are well conserved in evolution, predicted from corresponding genomes in *C. elegans* and *Drosophila* orthologs, which show closest homology to *mSesn1* (Budanov et al., 2002). In mammals, 3 Sestrin homologs are known while *Drosophila* and *C. elegans* only have a single form of Sestrin (Lee et al., 2010). Different forms of Sestrins in mammals show the most conservation in the α helical regions, which also contain multiple potential serine/threonine and tyrosine phosphorylation sites (Budanov et al., 2002). Further investigation of the *Hi95/mSesn2* gene indicated that it has close homology to *Mycobacterium tuberculosis* enzyme AhpD, which is an enzyme that catalyzes the reduction of the peroxiredoxin AhpC (Budanov et al., 2004). Peroxiredoxins are a family of thiol-containing peroxidases well conserved from bacteria to mammals and is known to play a role in catalyzing the decomposition of reactive nitrogen species (Budanov et al., 2004). The reduction of peroxiredoxins is important because the cysteine residue becomes oxidized to Cys-SO_2H under high oxidative stress conditions, which forms an inactive form of peroxiredoxin (Budanov et al., 2004). Overexpression of *Hi95/mSesn2* leads to a notable reduction of reactive oxygen species (ROS) in H_2O_2 treated cells while siRNA designed against *Hi95/mSesn2* results in an increased reactive oxygen species formation (Budanov et al., 2004). It was also shown that the conserved Cys^{125} of *Hi95/mSesn2* and Cys^{130} of *PA26/mSesn1* is important for the enzymatic function of Sestrins as the substitution of the Cysteine residues with Serine resulted in complete loss of the ability to decrease reactive oxygen species (Budanov et al., 2004). It was of interest that Sestrins are p53 responsive, which is a well-known tumor suppressosr

known to induce regulated cell cycle arrest and apoptosis (Velasco-Miguel et al., 1999). Another pathway known to be involved in cell growth is the previously described TOR signaling pathway. In addition, previous work suggested that Sestrins are induced upon hypoxia and DNA damage (Velasco-Miguel et al., 1999 and Budanov et al., 2002). Therefore, it was of interest whether Sestrins have a cytoprotective function by interacting with TOR to modulate cell growth and proliferation.

As mentioned previously, mTOR signaling is known to regulate cell growth and proliferation and is well conserved across species (Wullscheleger et al., 2004). The downstream targets of TOR signaling known to modulate cell growth include ribosomal protein p70S6K and 4E-BP. Therefore, phosphorylation levels of S6K and 4E-BP via western blot analysis allowed the assessment of the effect Sestrin plays in TOR signaling regulation (Budanov et al., 2008). It was verified using a doxycycline-OFF construct that Sestrin downregulates TOR signaling upon Sestrin induction, indicated by decreased phosphorylation of S6K and 4E-BP upon doxycycline removal (Budanov et al., 2008). In addition, this decreased TOR downstream target phosphorylation via Sestrin induction showed a similar pattern of TOR downregulation to rapamycin induced TOR inhibition (Budanov et al., 2008). Further investigation indicated that Sestrin acts through activation of AMPK, which then enhances the phosphorylation of TSC2 to inhibit Rheb and result in TOR downregulation (Budanov et al., 2008). The phosphorylation site on TSC2 by AMPK is different from the phosphorylation site on TSC2 by Akt and acts to upregulate the GAP activity of TSC2 to inactivate Rheb and downregulate TOR signaling (Towler et al., 2007). Recently, our lab showed the negative TOR regulatory function of Sestrin in the *Drosophila* model system (Lee et al., 2010). Tissue specific expression of InR and

Akt in the dorsal wing compartment resulted in a downward curved wing, indicative of enhanced cell growth in the dorsal wing compartment (Lee et al., 2010). The coexpression of Sestrin, however, reversed this phenotype and resulted in a wing phenotype more similar to wildtype wings (Lee et al., 2010). On the contrary, the loss of *dSesn* expression aggravated the downward curved wing phenotype in InR and Akt overexpressing organisms (Lee et al., 2010). In addition, the expression of components known to downregulate TOR signaling such as PTEN and TSC1/2 in the dorsal wing compartment results in upward curving of the wing, which is enhanced with coexpression of Sestrin (Lee et al., 2010). It is also interesting to note that this cell growth regulation via TOR signaling regulation takes place while maintaining the same number of cells in the dorsal wing compartment (Lee et al., 2010). This result was further verified by expressing InR^{CA} and *Rheb* along with *dSesn* overexpression lines in the eye using *gmr-GAL4* drivers to assess the effect dSesn plays in downregulating the hypertrophy phenotype observed under insulin receptor pathway mediated TOR activation (Lee et al., 2010).

Although the role Sestrin plays in TOR signaling regulation appeared clear, the physiological role that Sestrin plays in the organism was still not investigated. One of the downstream targets of TOR, SREBP, was suggested to mediate the lipogenic activity of TOR (Porstmann et al., 2008). Therefore, it was a question of interest to investigate whether the loss of Sestrin has an effect on lipid accumulation in *Drosophila*. *Drosophila* lacking the genomic expression of Sestrin ($dSesn^{-/-}$) was obtained by imprecise excision via *Δ2-3 transposase* by Lee et al., which was verified by southern blot analysis (Lee et al., 2010). The Sestrin null organisms were compared with wildtype organisms in

assessing the triglyceride levels in 3rd instar larvae fat bodies. The different densities of the fat cells were also assessed by Nile Red staining 3rd instar larvae fat bodies for wildtype and *dSesn*$^{-/-}$ organisms. The wildtype and *dSesn*$^{-/-}$ fat bodies were further analysed by western blot analysis measuring phosphorylation level of TOR targets.

As described before, one of the downstream targets of TOR is Atg1 and Atg13, which prevents the cell from entering autophagy under nutrient rich conditions (Chan et al., 2009). Autophagy can be divided into three different subtypes of processes: macroautophagy, microautophagy, and chaperone-mediated autophagy (Mizushima, 2007). The term autophagy we refer to from here on will be describing macroautophagy, unless mentioned otherwise. Autophagy is a highly regulated process involving many autophagy related genes (*Atg*), which become activated in an adaptive catabolic process in response to different forms of metabolic stress, including nutrient deprivation, growth factor depletion, and hypoxia (Levine et al., 2008, McPhee et al., 2009, and Mizushima, 2007). The release of amino acids and other nutrients such as free fatty acids from this autonomous digestion allows for such materials to be recycled and used to maintain cell survival in cases of nutrient deprivation (Levine et al., 2008). In addition to cytoprotective functions in cases of nutrient deprivation or cases of increased metabolic demands, defects in autophagic processes is reported to be involved in different disease pathogenesis such as neurodegenerative diseases, liver disease, myopathy, cardiac disease, and cancer (Levine et al., 2008, Mizushima, 2007, Wang et al., 2009, Pan et al., 2008, Hara et al., 2006, and Kundu et al., 2007). It was noted that the *dSesn*$^{-/-}$ organisms showed defective cardiac function when compared with wildtype organisms by having increased arrhythmia and decreased heart rate (Lee et al., 2010). Therefore, it was of

question whether decreased autophagy or the influence of other downstream components of the TOR signaling cascade is responsible for this phenotype. The two TOR cascade target components selected in an attempt to rescue the *dSesn-null* phenotypes were Atg1 and a constitutively active form of 4E-BP. This experimental setting allowed assessing whether cell translational overactivation or autophagy inhibition is responsible for the damaged cardiac performance observed in *dSesn-null* organisms.

There are no known characteristic signature domains in the Sestrin gene that allows the localization of the functional domain of the protein (Budanov et al., 2008). Although it has been shown that the N-terminal region and C-terminal region is important for mSesn2 functionality, it does not provide a clear localization of the functional domain since the construct was an artificially induced mutant by using primers designed to flank the N-terminal and C-terminal (Budanov et al., 2008). Therefore, it was questioned whether inducing random mutagenesis in the gene and screening for phenotypic alterations may allow the isolation of domain regions that provide protein functionality. As performed previously in our lab, two different systems were used to mutagenize *dSesn* and *mSesn1* using a *Δ2-3 transposase* and EMS mutagen respectively and expressed in a tissue specific manner to observe for altered cell growth patterns (Guichard et al., 2001).

Chapter 1: Study of Sestrin in cell growth, lipid metabolism, and cardiac physiology

Methods

Genotypes

Figure 2: (A) *gmr-GAL4*/+, (B) *gmr-GAL4; dSesn^{XP4}*/+, (C) *gmr-GAL4*/*UAS-InR^{CA}*, (D) *gmr-GAL4; dSesn^{XP4}*/*UAS-InR^{CA}*, (E) *gmr-GAL4*/*UAS-Rheb*, (F) *gmr-GAL4; dSesn^{XP4}*/*UAS-Rheb*, Genotypes in (G) was identical to the corresponding genotypes from (A) to (F). **Figure 3:** (A) *w^{1118}* and *dSesn$^{-/-}$*, (B) *dSesn$^{+/+}$, dSesn$^{-/-}$, dSesn$^{8A11/3F6}$, dSesn$^{+/-}$*; *hs-GAL4*/+, *dSesn$^{-/-}$*; *hs-GAL4*/+, *dSesn$^{-/-}$*; *hs-GAL4/UAS-Myc-dSesn^{WT}*, *dSesn$^{-/-}$*; *hs-GAL4*/*UAS-Myc-dSesn^{CS}, and dSesn$^{-/-}$ with respective drug treatments*, (C) *w^{1118},* and *dSesn$^{-/-}$* and (D) *w^{1118}* and *dSesn$^{-/-}$*. **Figure 4:** (A) *w^{1118}*, (B) *dSesn$^{-/-}$,* (C) *dSesn$^{-/-}$,* rapamycin, (D) *dSesn$^{-/-}$,* AICAR, (E) *dSesn$^{-/-}$,* Vitamin E, and (F – L) corresponds to respective genotypes from (A) – (E). **Figure 5:** (A) *UAS-GFP hand-GAL4/+,* (B) *dSesn-/-; UAS-GFP hand-GAL4/+,* (C) *dSesn$^{-/-}$; UAS-GFP hand-GAL4/UAS-Atg1,* (D) *dSesn$^{-/-}$; UAS-GFP hand-GAL4/UAS-Thor^{LL},* and (E – K) corresponds to the respective genotype from (A) – (D).

Drosophila eye assessment

The respective 10-day-old male flies of desired genotypes were collected and observed under Leica microscope. The images were taken under identical conditions for each respective genotype. Images were analyzed using imaging software (Adobe Photoshop).

Western blot analysis

When assessing the head proteins, 20 to 50 heads were collected from each fly of indicated genotype and the tissue was homogenized in cell lysis buffer (20 mM Tris-Cl pH 7.5, 150 mM NaCl, 1mM EDTA, 1 mM EGTA, 2.5 mM NaPPi, 1 mM β-glycerophosphate, 1 mM Na_3VO_4, 1% Triton-X-100). When assessing the larval fat body proteins, the fat bodies were dissected from 10 third instar larvae and homogenized in cell lysis buffer as described above. The insoluble fraction of the protein lysates were removed through centrifugation and the soluble fraction was boiled in 1X SDS sample buffer. The lysates were resolved by SDS-PAGE, transferred to PVDF membranes and protein bands probed with respective antibodies. Bands were detected using chemiluminescence assay in Versadoc system (Biorad). The intensity of the band was assessed from the inverted image, using the black background as reference. The band intensities were normalized against control for comparison.

Lipid level assessment though Nile Red staining

Nile Red staining was performed as described (Grönke et al., 2007). The third instar larvae of wild type and *dSesn*$^{-/-}$ flies were collected and the adipose tissue dissected out of them. The tissue was then fixed for 1 minute in Brower's fix solution, applied Nile Red staining for 3 minutes, washed 3 times using PBS for 1 minute each and then covered using a cover slip to observe under the microscope. The coverslip was placed while using waste tissues to support the edges of the coverslip to prevent the fat bodies from being squeezed.

Triglyceride level measurement

Crude lysates of 5-day-old adult males were prepared by sonication in PBS. The tryglyceride levels were measured using Triglyceride-SL assay kit (Genzyme Diagnostics) according to the manufacturer's instructions. The normalized protein levels were measureing according to the Biorad protein assay kit (Biorad).

Drug treatment

Metformin (Sigma), 5-aminoimidazole-4-carboxamide-1-β-Dribofuranoside (AICAR, TRC chemicals) and rapamycin (LLC chemicals) were dissolved in 300μL PBS to produce 100mM solution for AICAR and metformin and 1μM solution for rapamycin. The drugs were then given to the flies by mixing with the normal food. Vitamin E was dissolved in ethyl acetate and was mixed with normal food at 20μg/mL and allowed to dry in room temperature to eliminate the solvent odor.

Cardiac function assessment

The female flies were collected and allowed to age for two weeks in fresh food. The flies were then anesthetized in Flynap (Carolina Biological Supply Company) and placed on a small Petri dish using Vaseline to hold the flies with its ventral side facing up. The flies were then immersed in hemolymph made as described for preparation (Ocorr et al., 2007). The fly heart was then cleanly prepared using a micropipette connected to a vacuum while paying close attention not to touch the heart. Once the heart was clearly visible, the heartbeat was recorded for 1 minute under Hamamatsu CCD camera on a Leica DM LFSA microscope with a 10x dipping immersion lens. The

images were then processed using a PCI imaging software provided by Hamamatsu Inc. The processed images were then used to generate M-mode images using a MATLAB algorithm (Ocorr et al., 2007). The heart arrythmia index was determined by calculating the standard deviation of heartbeats. The heart rate was determined by calculating the mean heart rate of the flies with identical genotypes.

Results

Sestrin inhibits TOR signaling in Drosophila eye

Insulin signaling cascade activators such as Akt and Rheb were shown to result in activation of TOR signaling that promotes cell growth, indicated by increased downstream phosphoryaltion of S6K and 4E-BP (Budanov et al., 2008). In addition, genetic interaction studies in *Drosophila* wing indicates that expression of insulin receptor signaling activators such as constitutively active form of insulin receptor (InR), constitutively active form of PI3K ($PI3K^{CA}$) and *Akt* in the dorsal wing compartment result in downward curved wings, indicative of hypertrophy in the dorsal wing compartment (Lee et al., 2010). Therefore, it was questioned whether such phenotype can be observed in other organs in a tissue specific manner. Genetic interaction studies were performed using eye-specific *gmr-GAL4* driver to express the genetic components. Control eye phenotype with *gmr-GAL4* driver showed normal sized eye and *dSesn* overexpression produced only a slight reduction in eye and omatidia size (Figure 2A and 2B). However, when TOR signaling activators such as InR^{CA} and *Rheb* was expressed in the eye, the eye showed significant hypertrophy due to increased TOR activity as measured by increased phosphorylation of S6K and 4E-BP (Figure 2C, 2E and 2G).

Interestingly, Sestrin coexpression dramatically reduced the InR^{CA} and *Rheb* induced hyper-growth phenotype of the eyes (Figure 2D, 2F). Increased phosphorylation of S6K and 4E-BP by InR^{CA} and *Rheb*, which are indicators of increased TOR activity, were also decreased by *Sestrin* coexpression (Figure 2G). This indicates that Sestrin can inhibit InR and Rheb mediated eye growth by downregulating TOR signaling.

Loss of Sestrin in flies result in increased lipid accumulation

Nile Red staining was performed in wildtype and $dSesn^{-/-}$ fat bodies collected from 3rd instar larve to investigate the role of Sestrin in regulating lipid metabolism in *Drosophila* fat bodies. Nile Red is a lipophilic dye that allows identification of lipid droplets. In addition, the intensity of fluorescent signal can be used to quantify the amount of lipid in each droplet (Genicot et al., 2004). Upon analysis, the Nile Red staining of the $dSesn^{-/-}$ fat bodies show a greater intensity level when compared to wildtype staining performed and measured under identical conditions (Figure 3A). In addition, the measurement of triglyceride levels in wildtype and $dSesn^{-/-}$ adults show an increased level of triglycerides in $dSesn^{-/-}$ organisms compared to wildtype (Figure 3B). Analysis shows that the expression of *dSesn* results in dramatic decrease in triglyceride levels compared to *dSesn-null* organisms (Figure 3B). In addition, the expression of $dSesn^{CS}$, which has a mutated cysteine residue known to be important for reducing reactive oxygen species (ROS) was able to restore the triglyceride metabolism defects of $dSesn^{-/-}$ organisms as well as the expression of wildtype *dSesn* (Figure 3B). This indicates that the cysteine reside crucial for reducing ROS is not important for regulating lipid metabolism. Since Sestrin controls AMPK/TOR signaling independently of its redox

activity (Budanov et al., 2004), and because AMPK/TOR can regulate lipid metabolism through Serine Response Element Binding Protein (SREBP) transcription factor, we suspected that AMPK/TOR activity may be misregulated in fat bodies of *dSesn*$^{-/-}$ organisms. Indeed, western blot analysis showed that *dSesn*$^{-/-}$ fat bodies show increased S6K phosphorylation, increased 4E-BP phosphorylation, and decreased AMPK phosphorylation (Figure 3C and 3D). Decreased AMPK activity and increased TOR activity can cause lipid accumulation phenotype in diverse organisms (Porstmann et al., 2008). Feeding the *dSesn* null flies with AMPK signaling activators, such as AICAR, or TOR signaling inhibitor, rapamycin, also partially restored the lipid metabolism defects of *dSesn*$^{-/-}$ organisms (Figure 3B). This pharmacological result also confirms that Sestrin is regulating lipid meabolism by modulating the activity of AMPK and TOR signaling.

Hyperactive TOR signaling results in altered cardiac physiology

It was shown that dSesn null organisms show decreased heart rate and increased arrhythmia when compared to wildtype organisms (Lee et al., 2010; Figure 4A, 4B, 4F, and 4H). In addition, the *dSesn*$^{-/-}$ heart showed slightly increased diastolic and systolic diameter (Lee et al., 2010; Figure 4K and 4L). The cardiac phenotype observed in *dSesn-null* organisms was verified to be due to decreased AMPK and increased TOR signaling since feeding *dSesn-null* organisms AICAR or rapamycin resulted in rescue of heart rate, decreased arrhythmia index and a reduction in diastolic diameter (Lee et al., 2010; Figure 4C, 4D, 4F, 4H, 4K and 4L). While the heart rate was rescued when *dSesn-null* organisms were fed with rapamycin and AICAR along with their normal diet, catalase overexpression or feeding vitamin E, which is known to reduce ROS, did not affect heart

rate (Lee et al., 2010; Figure 4E, 4F and4H), however, did show an improvement in reducing arrhythmicity index. TOR was known to suppress translation and induce autophagy, both of which can affect cardiac physiology (Lee et al., 2010). Two TOR downstream target genes were expressed specifically in the heart using the *hand-GAL4* driver (Lee et al., 2010) to investigate which branch of the TOR signaling pathway is responsible for *Drosophila* cardiac physiology regulation. Two TOR downstream targets selected were *Atg1*, an autophagy initiating protein kinase that is inhibited by TOR phosphorylation and 4E-BP, and a constitutively active 4E-BP ($Thor^{LL}$), which suppresses translation. Interestingly, while *Atg1* overexpression did not show an improvement in heart rate, $Thor^{LL}$ expression showed a slight rescue of heart rate indicated by significantly decreased diastolic interval to a normal level (Figure 5E, and 5I). Therefore, it was suspected that the translational control of TOR is critical for maintaining heart period. Consistent with this idea is that increased protein translation by 4E-BP mutation, TOR activation, or eIF4E expression in heart caused increased heart period in *Drosophila* model (Wessells et al., 2009). Although $Thor^{LL}$ overexpression restored $dSesn^{-/-}$ defect in heart period, it was unable to restore the arrhythmic index since the $dSesn^{-/-}$ heart with $Thor^{LL}$ expression show similar arrhythmia with $dSesn^{-/-}$ control heart (Figure 5H). This finding partly supports the theory that ROS may be responsible for arrhythmia while suppression of translational activity is more involved in restoring the heart rate defects. It has been known that deceased autophagy can increase dysfunctional mitochondria, thereby generating more ROS (Chan, 2009). TOR, as an autophgy suppressor can increase ROS. Therefore, the arrhythmicity observed in $dSesn^{-/-}$ organisms may be attributed to the inability to remove ROS due to suppressed autophagy

through hyperactive TOR activity. However, *Atg1* overexpression in *dSesn*$^{-/-}$ heart was unable to restore the heart rate defect but rather aggravated arrhythmicity of the *dSesn*$^{-/-}$ heart (Figure 5D and 5H). The adverse effect of overexpressing *Atg1* may indicate that too much autophagy may actually cause tissue damage (Mizushima, 2007). Therefore, this would indicate that a more intricate network of autophagy control is necessary to have a beneficial effect in reducing ROS and rescuing the arrhythmicity. Increased autophagy and decreased protein translation both result in suppression of the increased diastolic diameter phenotype of *dSesn*$^{-/-}$ organisms (Figure 5K and 5L). This result is consistent with the previous findings that enhanced autophagy and reduced protein translation results in decreased tissue growth (Chan, 2009). While *Atg1* overexpression was not effected in restoring *dSesn*$^{-/-}$ cardiac defects, silencing of *Atg1* in heart by *hand-GAL4/Atg1-RNAi* transgene resulted in increased heart period, arrhythmicity and increased cardiac diameter (Lee et al., 2010). This indicates that defective autophagy in *dSesn*$^{-/-}$ heart may be responsible for aggravating the defect primarily caused by defective protein translation and ROS regulation.

Discussion

Sestrin mediated regulation of AMPK-TOR signaling has been well documented in literature, but the physiological meaning of that regulation was elusive. In this study, I investigated the role of Sestrin in *Drosophila* eye omatidia, fat body and heart. In *Drosophila* eye, although Sestrin-dependent growth reduction was not pronounced in wildtype background, Sestrin was able to reduce the growth-promoting effect of TOR signaling activators including InR^{CA} and Rheb by inhibiting TOR activation. This

indicates that the negative growth regulatory function of Sestrin may be more important in the context of TOR hyperactivation, which may cause increased metabolic and oxidative stress. Our lab has recently published the results indicating that Sestrin induction is triggered upon increased oxidative stress and is mediated through the JNK-FoxO pathway (Lee et al., 2010). Therefore, Sestrin may be playing a cytoprotective role in the cell to reduce metabolic damage induced upon increased ROS, resulting from TOR hyperactivation.

The role Sestrin plays in regulating metabolic processes such as lipid accumulation was assessed using a *dSesn* knockout mutant (Lee et al., 2010). Such analysis resulted in the findings that *dSesn* knockout organisms have increased levels of lipid droplet accumulation, possibly, due to increased TOR signaling activity. This finding was further verified by assessing the *dSREBP* target lipogenic genes through quantitative PCR analysis, which indicated that lipogenic gene transcription was enhanced while lipolytic gene transcription was reduced (Lee et al., 2010). The TOR signaling cascade is intricately connected to the insulin signaling pathways through Akt and TSC1/2 (Wullschleger et al., 2006). Therefore, such TOR hyperactivation-mediated lipid accumulation shows a close relationship to metabolic diseases such as obesity, which are conditions resulting from nutrient over-consumption and is observed in developed countries at increasing rates. Obesity is especially becoming a growing problem in developed nations and is attributed to shortened lifespan (Harrison et al., 2009). Recent report by Harrison et al., indicating rapamycin feeding to mice extends lifespan, supports the theory that TOR hyperactivity-mediated metabolic disease attributes to lifespan shortening (Harrison et al., 2009). Therefore it is of interest what

physiological role Sestrin plays in different tissues as a TOR regulatory cytoprotective molecule and how it affects the longevity of the organism.

The physiological role of Sestrin assessed by analyzing *Drosophila* cardiac mechanics also indicates that Sestrin-mediated TOR regulation is an important component in proper cardiac physiology. Analysis indicates that *dSesn-null* organisms have a reduced heart rate and increased level of arrhythmicity along with increased tissue diastolic diameter. This decreased heart rate was rescued upon AICAR or rapamycin administration, which indicates that TOR hyperactivation is responsible for the $dSesn^{-/-}$ heart defects. TOR hyperactivation is also known to cause an increase in ROS, which can be reduced through the expression of catalase or vitamin E (Lee et al., 2010). Upon ROS reduction, the *dSesn*-null organisms showed reduced arrhythmicity, however, did not have an effect on heart rate. The cardiac function rescue of *dSesn-null* organisms was attempted through the expression of two TOR downstream components, *Atg1* and constitutively active 4E-BP. The expression of 4E-BP showed a slight rescue of heart rate while *Atg1* overexpression had no significant effect on heart rate. The overexpression of *Atg1* had an adverse effect on arrhythmicity while 4E-BP had little effect on arrhythmicity. The expression of both components resulted in reduction in diastolic diameter. Autophagy was expected to reduce arrhythmia by reducing ROS in cardiac cells. However, *Atg1* overexpressin $dSesn^{-/-}$ heart actually resulted in worsened arrhythmia index. This result can be interpreted in different angles. First, it may be possible that simple overexpression of autophagy regulatory genes does not result in cytoprotective autophagy induction. It is possible that too much autophagy can cause damage to the cells (Levine et al., 2008). Therefore, it may be that the intricate regulation

of the multiple autophagy regulatory genes is necessary to induce cytoprotective autophagy and cause ROS reduction. Second, the phosphorylation sites of Atg1 by TOR are still unclear. Therefore, it is possible that the hyperactive TOR signaling in *dSesn-null* organisms can still inhibit the exogenous Atg1 being expressed. The combination of TOR hyperactivation and *Atg1* overexpression may be contributing to the adverse cardiac rhythm observed. It is unclear at this point how autophagy mediates the cardiac mechanics under TOR hyperactive conditions and would require further investigation.

As mentioned before, it is interesting to note that the hyperactive TOR-mediated pathophysiological effects such as lipid accumulation and dysfunctional cardiac mechanics are similar to those observed in people of developed nations with increasing frequency due to nutrition over-consumption and aging (Poireier et al., 2006). Increasing number of evidence suggests that TOR hyperactivation is responsible for numerous human diseases such as cardiovascular disease, neuronal degeneration, obesity and cancer (Hay et al., 2004, Martin et al., 2005, Wullschleger et al., 2006, and Lee et al., 2010). It has also been known for several years that TOR controls reproductive lifespan in worms and *Drosophila* and the lifespan of the organisms can be extended by nutrient limitation (caloric restriction), connecting nutrient sensing pathways and aging (Martin et al., 2005).

The dSesn mediated TOR signaling regulation in the eye omatidia, lipid physiology and regulation of lipogenic/lipolytic genes, and cardiac recording experiments in Figure 4 and Figure 6 contains reproduced published data by Lee J. H., Budanov A. V., Park E. J., Birse R., Kim T. E., Perkins G. A., Ocorr K., Ellisman M. H., Bodmer R., Bier E., and Karin M. in Science 2010.

Chapter 2: NOVA screening of *dSesn* and *mSesn1*

Methods

Genotypes

Figure 7: *w^+ Δ2-3*, *UAS-dSesn*, *gmr-GAL4*. **Figure 11:** *ap-GAL4*/*In(2LR), Bc*, *Gla*, *UAS-mSesn1*/*In(2LR), Bc, Gla*.

Genetic crosses and fly stocks in dSesn screen

Drosophila melanogaster with w^{1118} background were used throughout this study. NOVA screening was performed as described in our lab's previous paper (Guicard et al., 2001). In detail, *UAS-dSesn* males were crossed with *w^+Δ2-3 transposase* line virgins to generate non-specific mutations in the target gene, resulting in flies with *UAS-dSesn/w^+Δ2-3* genotype. This generates random P-element excisions that generate mutations in the genome. Males from the F1 progeny were collected and then crossed to eye-specific driver, *gmr-GAL4*, to select candidate mutants based on its effects on eye size control. Candidate mutants with red eyes were selected and screened for any alterations in eye size. A loss of function mutation would result in an increased eye size while a gain of function mutation would result in a decreased eye size. Approximately 50,000 target organisms were assessed to select the candidate mutants. Following the primary screen using *gmr-GAL4* driver, crossing the candidate mutants to the wing-specific driver, *ap-GAL4*, allowed further assessment in its effects on cell growth control. In the wing, gain of function or loss of function mutation was assessed by observing at the wing curvature. The genetic scheme was performed as outlined in Figure 7.

DNA extraction and sequencing

DNA samples were extracted using the DNeasy blood and tissue kit and was performed according to manufacturer's protocol (Qiagen). Specific genomic fragments were amplified by PCR and the PCR products were analyzed by standard DNA sequencing (Eton Bioscience).

Candidate selection and Molecular analysis of candidate dSesn mutant

The organisms that exhibit altered eye growth phenotypes, larger or smaller eye, compared to the control were isolated and used for further investigation. Polymerase chain reaction (PCR) analysis was performed, using primers designed to flank the UAS site to the *dSesn* insertion forward 5' - CGT CTA CGG AGC GAC AAT TC - 3' and reverse 5' - TGG CAG ATT TCA GTA GTT GCA G - 3'. Additionally, a primer designed to flank the entire vector insertion from the *UAS* site to the w^+ was designed, forward 5' - CGT CGA CGG AGC GAC AAT GC - 3' and reverse 5' - ATT CAG TGC ACG TTT GCT TG - 3', to identify the presence of total deletion. Comparing the candidate sequence to the original *UAS-dSesn* insertion sequence allowed assessing the presence of deletion.

Acridine-Orange staining

Acridine-Orange solution was diluted to 10µg/mL in 0.1M PBS. The eye imaginal disk was isolated from 3rd instar larve of respective genotype. The tissue was stained with acridine orange staining for 1 minute and then washed with PBS 3 times, 1 minute each. The coverslip was placed while using waste tissues such as the epidermis to support the

edges of the coverslip to prevent the imaginal discs from being squeezed. The stained tissue for wildtype and *dSesn*$^{-/-}$ was observed under the fluorescent microscope and processed using imaging software (Adobe).

Inverse PCR

Inverse PCR was performed as designed according to the modified standard protocol originally described by Berkeley Drosophila Genome Project (BDGP). 30 flies were collected and DNA was extracted using DNeasy blood and tissue kit (Quiagen). The DNA was then digested by mixing 10µl DNA, 2.5µl 10X buffer, 2.0µl 100µg/ml RNase, 8.0µl ddH_2O and 10 units of restriction enzyme. Restriction enzymes Msp1 and HinP1 were used for this experiment. The mixture was incubated at 37°C for 2.5 hours. The enzyme was inactivated at 65°C for 20 minutes. The DNA was then ligated by mixing 10µl of digested DNA, 40µl of 10X ligation buffer, 350µl of ddH_2O, and 2.0µl of ligase. This mixture was then incubated overnight at 4°C. The DNA was then ethanol precipitated on ice for 10 minutes. Spin, aspirate, pulse, aspirate was repeated. The pellet was dried and resuspended in 150µl TE. PCR reactions were set up by mixing 10µl of ligated genomic DNA, 8.0µl of dNTP, 1.0µl of forward primer, 1.0µl of reverse primer, 5.0µl of 10x Taq buffer, 31.0µl of ddH_2O and 0.4µl of Taq. Forward primer used was 5' - GAC ACT CAG AAT ACT ATT C - 3' and reverse primer used was 5' - GCA TCA CAA AAA TCG ACG CTC AAG T - 3'. PCR results were resolved and eluted (Qiagen). Inverse PCR products were analyzed by standard DNA sequencing (Eton Bioscience). Sequenced DNA was then analyzed using Genebrowser (Flybase).

Sequence alignment

The candidate mutant sequences were aligned using basic local alignment search tool (BLAST) for the inverse PCR result in *dSesn* mutagenesis. The DNA sequence was first translated and protein sequence aligned for the *mSesn1* mutagenesis screen. The aligned protein sequence was then subjected to a protein BLAST algorithm to isolate potential mutations.

Ethane methyl sulfonate (EMS) mutagenesis

UAS-mSesn1/Bc male flies were collected and starved for 8 hours. The flies were then transferred into a vial with padding damped with 2ml of EMS in 5% sucrose solution. Different EMS concentrations, 13µl, 25µl and 45µl in 5ml 5% sucrose solution, were used to generate mutants. Following mutagenesis, the flies were allowed to "wipe their feet" on clean padding and then allowed to recover for 1 hour in a fresh food vial. The males were then crossed with *ap-GAL4* virgins to generate *UAS-mSesn1*/ap-GAL4* flies. The genetic scheme is outlined in Figure 11.

Candidate selection

Looking for any alterations in the wing growth, mutants were isolated by observing the wing curvature, and wing size. Since *ap-GAL4* driver is only expressed on the dorsal side of the wing, wild type *UAS-mSesn1/ap-GAL4* yields a slight upward curve of the wing due to decreased growth. Therefore, candidates that showed enhanced curvature or diminished curvature of the wing were selected for further assessment and were labeled *UAS-mSesn1*/ap-GAL4*. Due to high variations in phenotypes, the

candidates were backcrossed to *ap-GAL4* to verify for its phenotype. The candidates that seemed to maintain the phenotype in the second cross were further analyzed by PCR and sequence analysis.

Molecular analysis of candidate mSesn1 mutant

Candidate mutant alleles were amplified by crossing to *ap-GAL4* and collected for molecular analysis. 5 flies with *UAS-mSesn1*/ap-GAL4* genotype were collected and its genomic DNA extracted for assessment using Qiagen DNeasy blood and tissue kit and performed according to manufacturer's specifications (Qiagen). PCR was performed using primer sequence 5' - GCG GAA TTC ATG CGC CTG GCC GCC G - 3' in the forward direction and 5' - CGC GGA TCC TCA GGT CAT ATA CCG GGT AAT GG - 3' in the reverse direction and the DNA was further purified using Qiagen gel extraction kit (Qiagen). Eluted DNA was then sequenced, translated to protein sequence, aligned to form the full-length protein and BLAST against the mouse protein database to observe for alterations in the amino acid sequence.

Results

Statistics and genetic schemes

Approximately 100,000 organisms were screened for dSesn mutant screening using *Δ2-3* transposase. The genetic mutations that may be caused by *Δ2-3* transposase are imprecise excisions around the P-element insertion site. Therefore, crossing *UAS-dSesn* with w^{+}*Δ2-3* will cause imprecise excision mutations around *UAS-dSesn* insertion sites. *UAS-dSesn/*w^{+}*Δ2-3* organisms were then crossed to *gmr-GAL4* virgins to screen for

mutated *UAS-dSesn.* Therefore, of the organisms screened, 50% were of the target genotype. This leaves 50,000 organisms out of the total 100,000 screened with the desired genotype. Approximately 70,000 organisms were screened for *mSesn1* mutant screening using EMS mutagen. EMS mutagen is known to induce point mutations every 150kbp (Bokel, 2008). Treatment of EMS to *UAS-mSesn1* mutants will generate point mutations that may cause frame shift mutations, change protein sequence, or produce early stop codon to from and truncate the protein sequence. Of course, the possibility of a silent mutation or a mutation being fixed by the organism's DNA repair machinery cannot be ignored as well. Mutated *UAS-mSesn1/Bc* was crossed to *ap-GAL4/Bc*. Therefore, 50% of the progenies were of the desired *UAS/mSesn1/ap-GAL4* genotype. This leaves 35,000 organisms of target genotype out of the total 70,000 organisms produced from the screen.

Identification of No-Eye-Female (NEF) phenotype

UAS-dSesn flies (Figure 8A) were mutagnized using a *Δ2-3 transposase* element and then crossed with eye specific driver, *gmr-GAL4*, to screen for presence of mutations. From the genetic screening, a mutant with dramatic loss of growth in the eye omatidia was observed (Figure 8C and 8D). This mutant was named *No-Eye-Female* (*NEF*). The isolated mutant was further purified to generate organisms carrying the *UAS-NEF* and *gmr-GAL4* driver on the same chromosome (Figure 8D) through recombination and mutants just carrying *UAS-NEF* (Figure 8B). The mutant carrying just *UAS-NEF* was verified to generate identical phenotypes when crossed with *gmr-GAL4* as those mutants carrying *UAS-NEF* and *gmr-GAL4* on the same chromosome (Figure 8C). Therefore, it

was verified that the no-eye phenotype observed in the *NEF* mutant was *UAS* dependent. It was questioned whether the expression of *UAS-NEF* would cause dramatic undergrowth when expressed in the dorsal wing compartment and cause a greater upward curved wing than wildtype *dSesn* expression. The *UAS-NEF* mutant was crossed to *ap-GAL4* to observe for its effects on the wing phenotype, however, produced no progeny due to lethality (data not shown).

Molecular analysis of NEF mutant

The mutation that took place in the *NEF* allele was characterized using PCR analysis. Primers were designed flanking the *UAS* site and *dSesn* insertion site (Figure 8E), however, was unsuccessful in yielding good PCR results (data not shown). Instead, the entire vector insertion from the *UAS* site to the w^+ region was used to determine the excised region of the vector through mutation (Figure 8F). The sequencing result suggested that the plasmid insertion had some remaining w^+ region and the *UAS* site intact, but the *dSesn* insertion totally excised (Figure 8G). Therefore, this suggested the mutant phenotype might be a result of the *UAS* region turning on a gene that is downstream of the insertion site instead of through a mutation in the *dSesn* gene.

Acridine-Orange staining

Cell death was not observed in *dSesn* overexpression organisms and hence it was questionable whether the mutant phenotype was a result of a mutant *Sestrin* or not. Upon acridine-orange staining, mutant organisms showed extensive cell death in the developing eye imaginal disk compared to control eye imaginal disks (Figure 9A and 9B). This

suggested that the *NEF* phenotype could potentially be a result of a different gene being turned on by the *UAS* element and not a modified *Sestrin* gene causing the phenotype. This result supported the findings from PCR characterization, which determined that the entire *dSesn* insertion was deleted. Further sequencing analysis and molecular characterization was required for mutant characterization.

Inverse PCR to determine unknown downstream gene

Since it was known that the w^+ region was still intact in the *NEF* allele, it was decided that primers designed at the end of the w^+ region be used to perform inverse PCR in an attempt to identify the gene being activated by the *UAS* element (Figure 10A). Only the use of HinP1 restriction enzyme yielded usable results (Figure 10B). Upon analysis, it was determined that the gene becoming activated downstream of the plasmid insertion site was *CG13393* (Figure 10C). This gene is also called *Defender-against-death-1* (*Dad-1*) and whether *NEF* phenotype is caused by *Dad-1* expression should be determined in the future.

Discussion

Analysis of the Sestrin protein indicates no known characteristic domains that may be responsible for protein-protein interaction. In addition, the structures of Sestrin proteins have not yet been characterized. Therefore, it was of interest to investigate specific domain function of the *Sestrin* gene through random mutagenesis. Randomly mutating the target gene and looking for phenotypic variation would allow the experimenter to localize specific domains responsible for Sestrin function without the

addition of artificial manipulation (Guichard et al., 2001). It was thought that multiple mutants would be isolated that would allow the narrowing of the domain that is responsible for protein functionality, however, not as many mutants were isolated as expected. In the case of EMS mutagenesis screen, the mutagen induces point mutations at a frequency of 1 every 150kbp. Since the *mSesn1* gene insertion is 1.5kbp, this provides a 1% chance that a point mutation would occur in the target sequence. This yields approximately 350 mutants out of the 35,000 target organisms screened through mutagenesis. However, DNA repair mechanisms may be able to repair the point mutation and also the point mutation may not necessarily cause a change in protein sequence. It is questionable whether screening more organisms may yield in isolating a mutant. Another confounding issue with the mutagenic screen was the mild and variable phenotype being observed for the screening. It is possible to refine the screen by coexpressing the candidate gene with TOR signaling components that enhance the reduction in cell growth phenotype.

The *NEF* mutant isolated from the *dSesn* mutagenesis screen was found to be caused by the expression of a downstream gene called *Dad-1*, which is a protein encoding gene that is thought to be involved in inhibiting apoptosis. The defined role of the protein was different from our findings so we attempted further characterization using different tissue specific drivers and performing genetic interaction studies with the insulin receptor pathway components genes (data not shown). These experiments generate no viable progenies due to toxicity. It may also be possible that the mutation caused unpredictable changes in the protein conformation, such as the generation of a fusion protein with the remaining parts of the *dSesn* insertion, which generated the mutant

phenotype in a neomorphic manner. Therefore, the project was terminated at this point and a different mutagenic study using *mSesn1* was performed using a pharmacological mutagen, EMS. The mutagenic study of *mSesn1* was thought to provide insightful information regarding Sestrin protein domains and allow for quick testing using mammalian cell cultures. The EMS mutagenesis study, however, failed to yield any mutants with altered *mSesn1* protein sequence. The sensitivity of the NOVA screening may be improved by using a more lethal driver to express the target gene that would normally kill the organisms, however, result in survival under loss of function mutations.

Figures

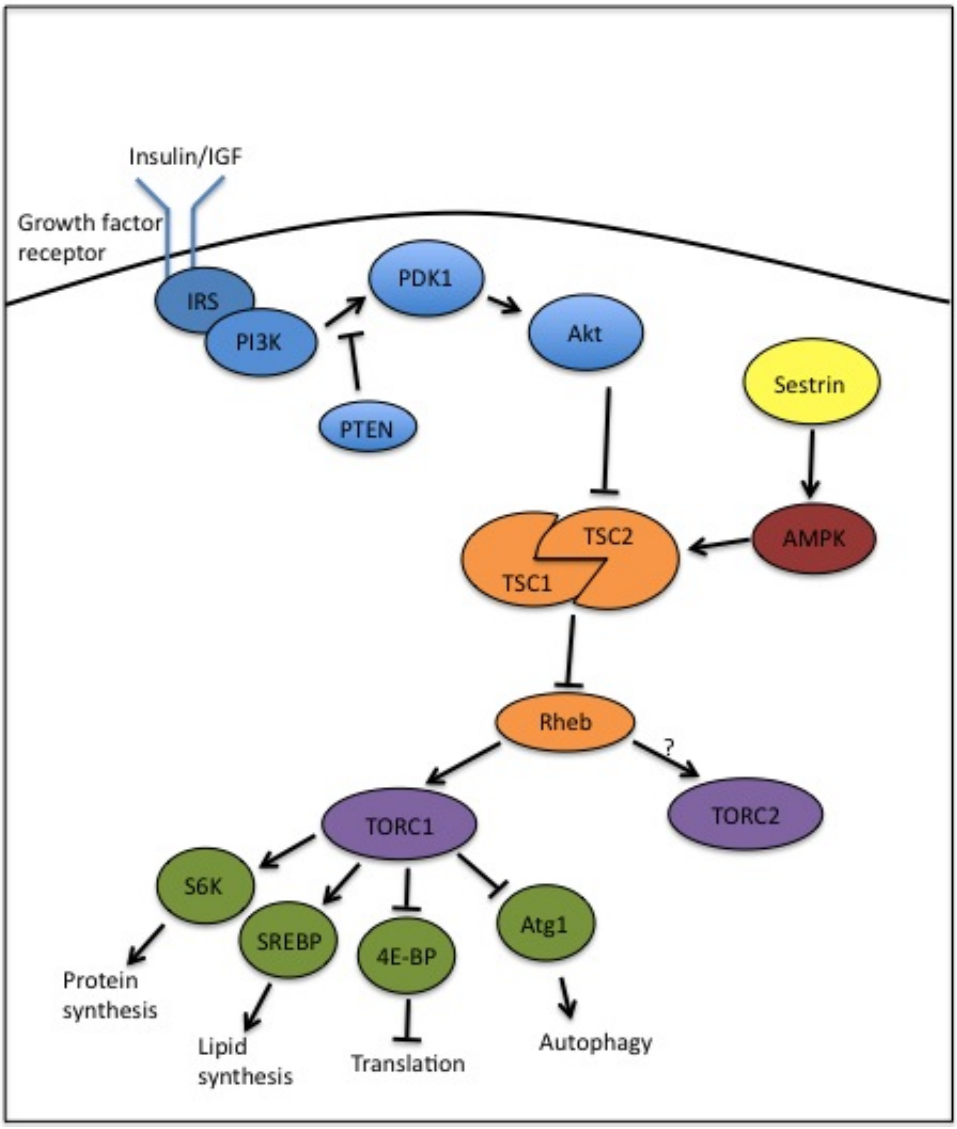

Figure 1: Insulin receptor mediated TOR signaling. The upstream and downstream components of TOR complex are summarized through Figure 1. Insulin signaling activation triggers the activation of PI3K. This forms phosphoinisitol-3-phosphate (PIP3) molecules, which recruits downstream components with pleckstrin homology (PH) domains, amongst which are PDK1 and Akt. Co-recruitment of PDK1 and Akt causes Akt activation by PDK1, which then phosphorylates TSC2. This prevents TSC1/2 heterodimer formation, which normally acts to activate Rheb-GTPase activity to inhibit TOR activation. In the absence of TSC1/2 heterodimer, Rheb-GTP binds to TORC1 to cause activation. TORC1 activation causes phosphorylation of S6K, activation of ribosome biosynthesis and transcription, while inhibiting 4E-BP and autophagy. We concentrated our investigation in TORC1, which is the TOR complex that is responsive to rapamycin.

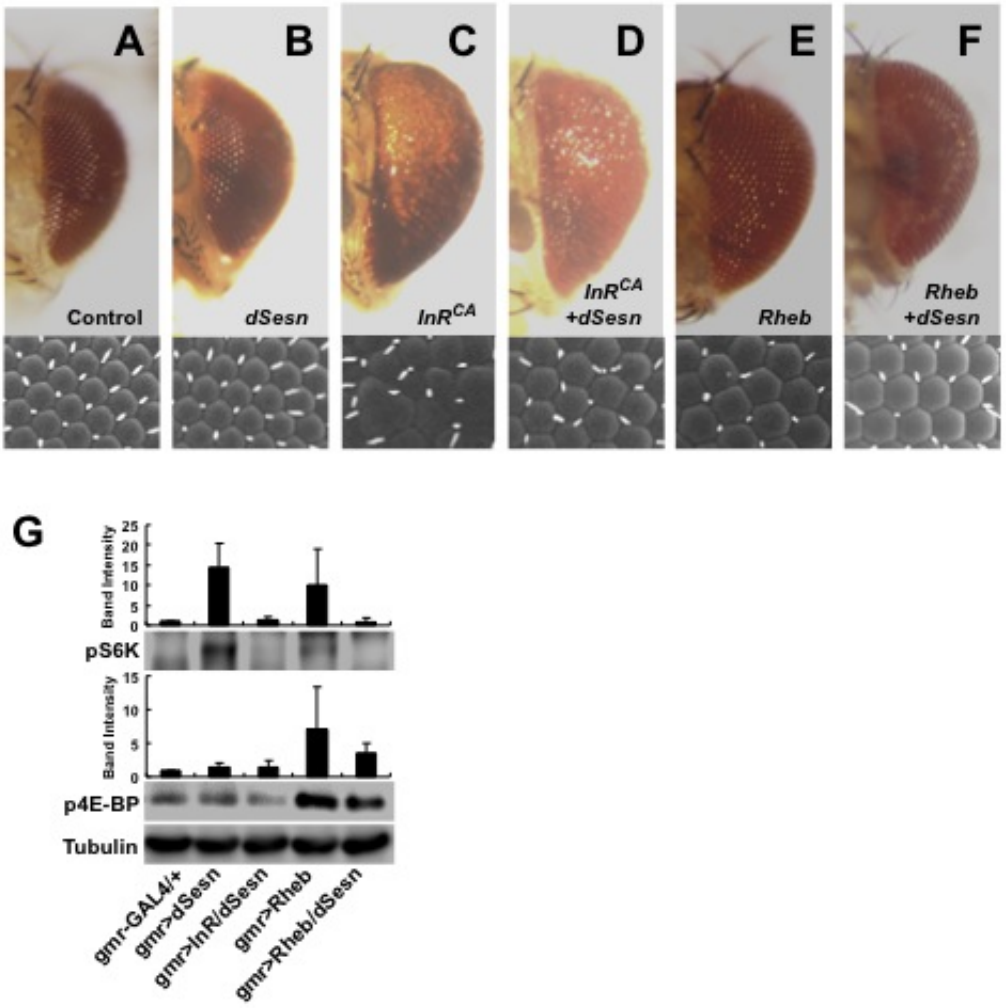

Figure 2: Genetic interaction of dSesn in eye omatidia. (A) *gmr-GAL4/+* control, (B) *gmr-GAL4, UAS-dSesn/+,* (C) *gmr-GAL4/InR*^{CA}, (D) *gmr-GAL4, UAS-dSesn/UAS-InR*^{CA}, (E) *gmr-GAL4/UAS-Rheb*, (F) *gmr-GAL4, UAS-dSesn/UAS-Rheb*. The expression of dSesn in eye omatidia only shows slight reduction in eye size when TOR is not hyperactive. However, expression of *dSesn* in TOR hyperactivation background resulted in significant reduction in tissue size when compared to TOR hyperactivation without *dSesn* expression (A – F). (G) The TOR signaling downregulation by *dSesn* is assessed by westernblot analysis.

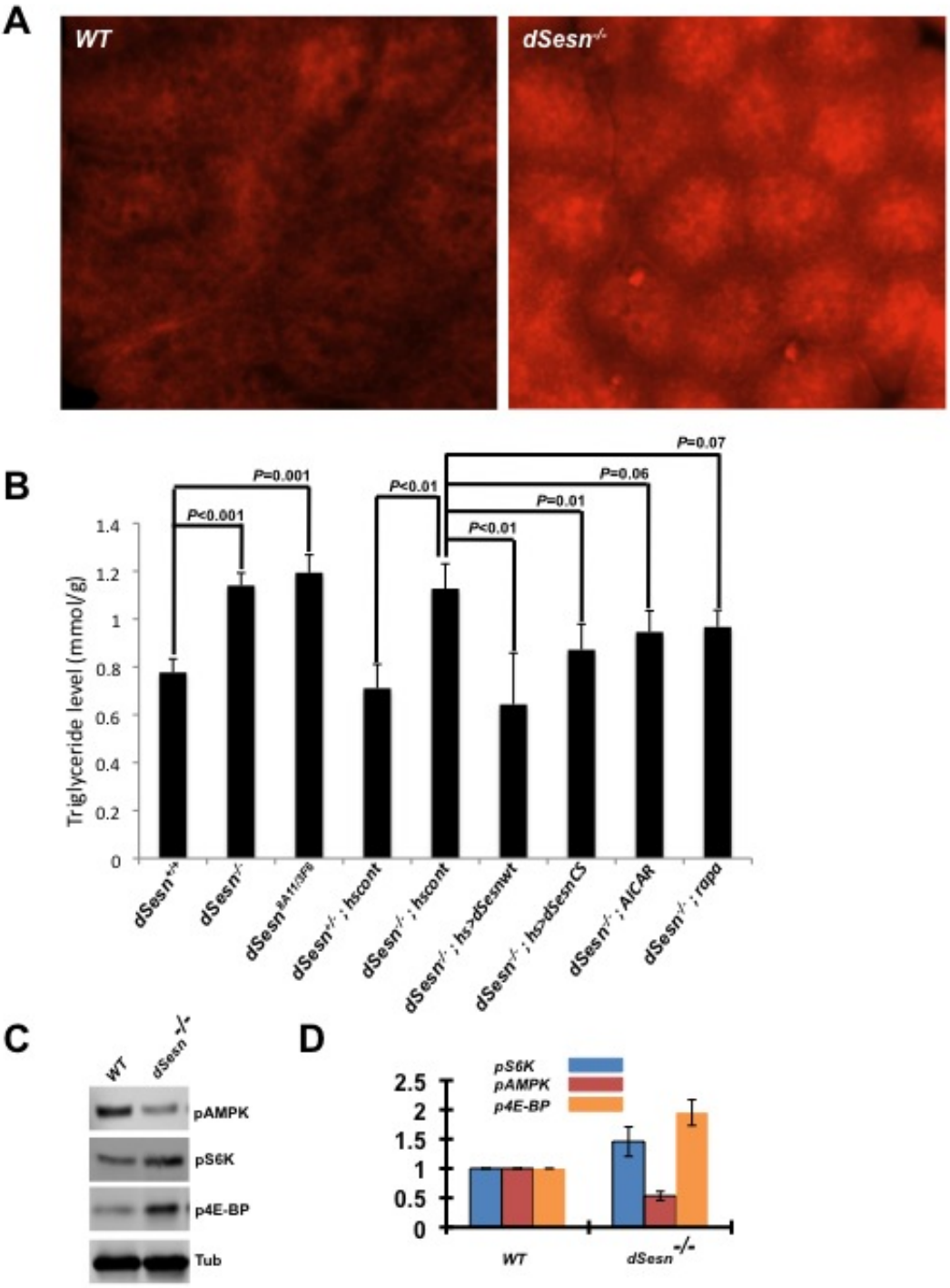

Figure 3: Increased lipid accumulations upon loss of *dSesn*. (A) Nile Red staining of wildtype and *dSesn-null* larval fat body, (B) Triglyceride level measurements for each respective genotype, (C) Western blot analysis of wildtype and *dSesn-null* larval fat body, (D) Western blot quantification.

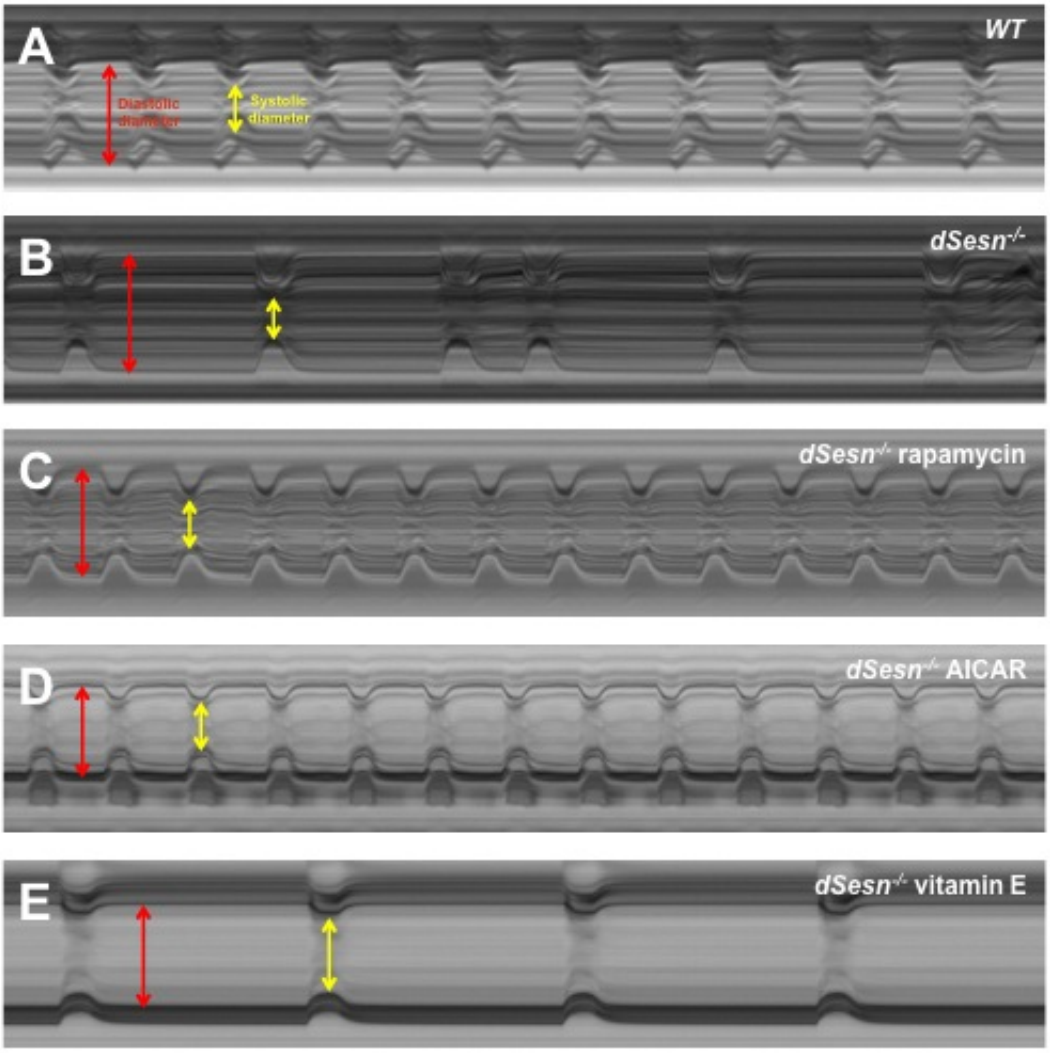

Figure 4: Wildtype and *dSesn-null* organism cardiac performance and rescue experiment. (A and B) Cardiac performance was compared between wildtype and *dSesn-null* organisms. (C) *dSesn-null* organism cardiac recording following rapamycin feeding. (D) *dSesn-null* organism cardiac recording following AICAR feeding. (E) *dSesn-null* organism cardiac recording following vitamin E feeding. The M-mode pictures are presented for each respective genotype. Panels indicate a short segment of the total 60 seconds image. Diastolic and systolic diameters are indicated by the red and yellow arrows respectively. (F – L) Parameters obtained from the matlab program was used to obtain heart rate, heart period, arrhythmicity, diastolic interval, systolic interval, diastolic diameter, and systolic diameter.

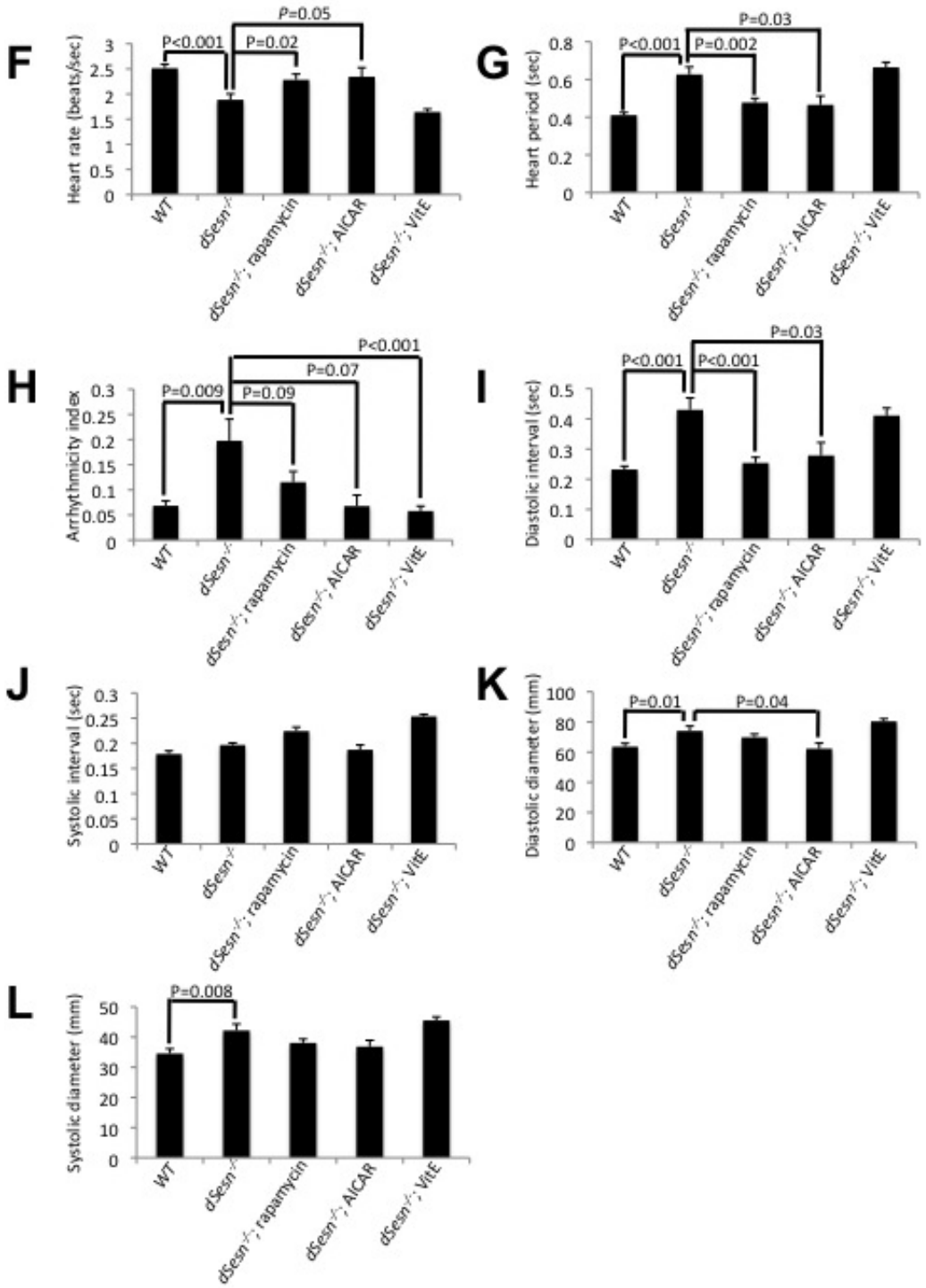

Figure 4: Continued.

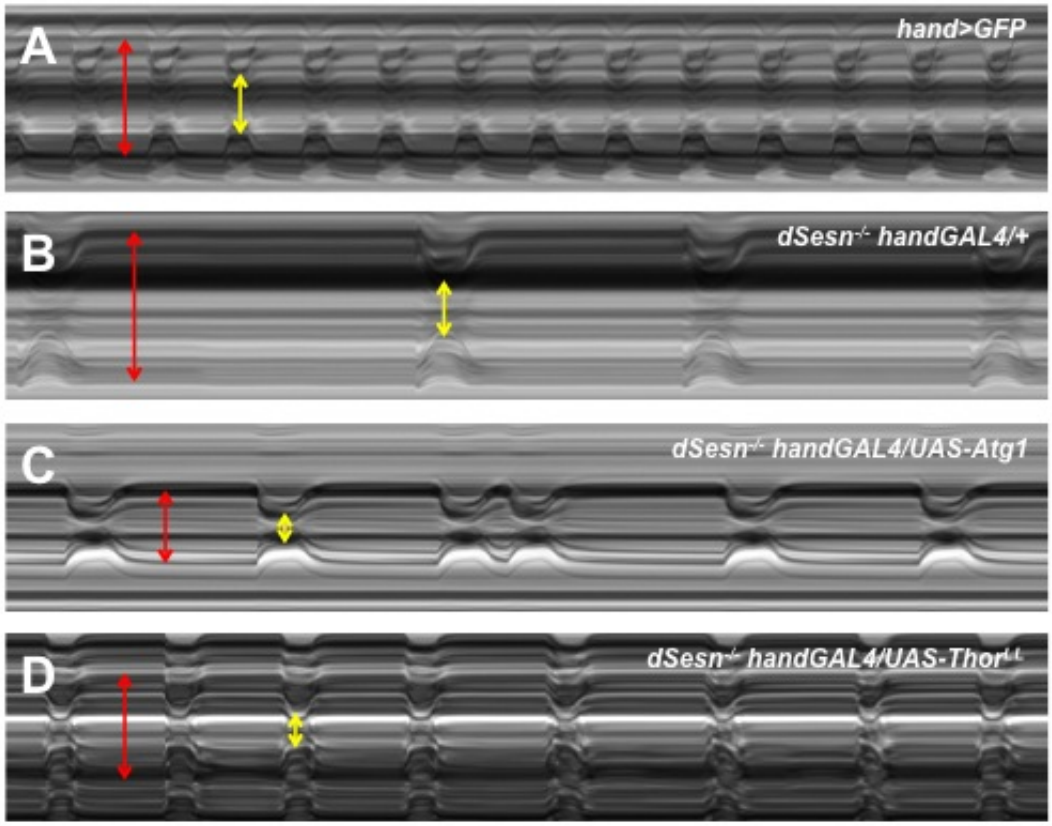

Figure 5: Tissue specific expressions of *Atg1* and *ThorLL* in rescuing *dSesn-null* cardiac function phenotype. (A) *hand-GAL4/+*, (B) *dSesn-null; hand-GAL4/+*, (C) *dSesn-null; hand-GAL4/UAS-Atg1,* and (D) *dSesn-null; hand-GAL4/UAS-ThorLL* cardiac recording. The M-mode pictures are presented for each respective genotype. Panels indicate a short segment of the total 60 seconds recording image. Diastolic and systolic diameters are indicated by the red and yellow arrows respectively. (E – K) Parameters obtained from the matlab program was used to obtain heart rate, heart period, arrhythmicity, diastolic interval, systolic interval, diastolic diameter, and systolic diameter.

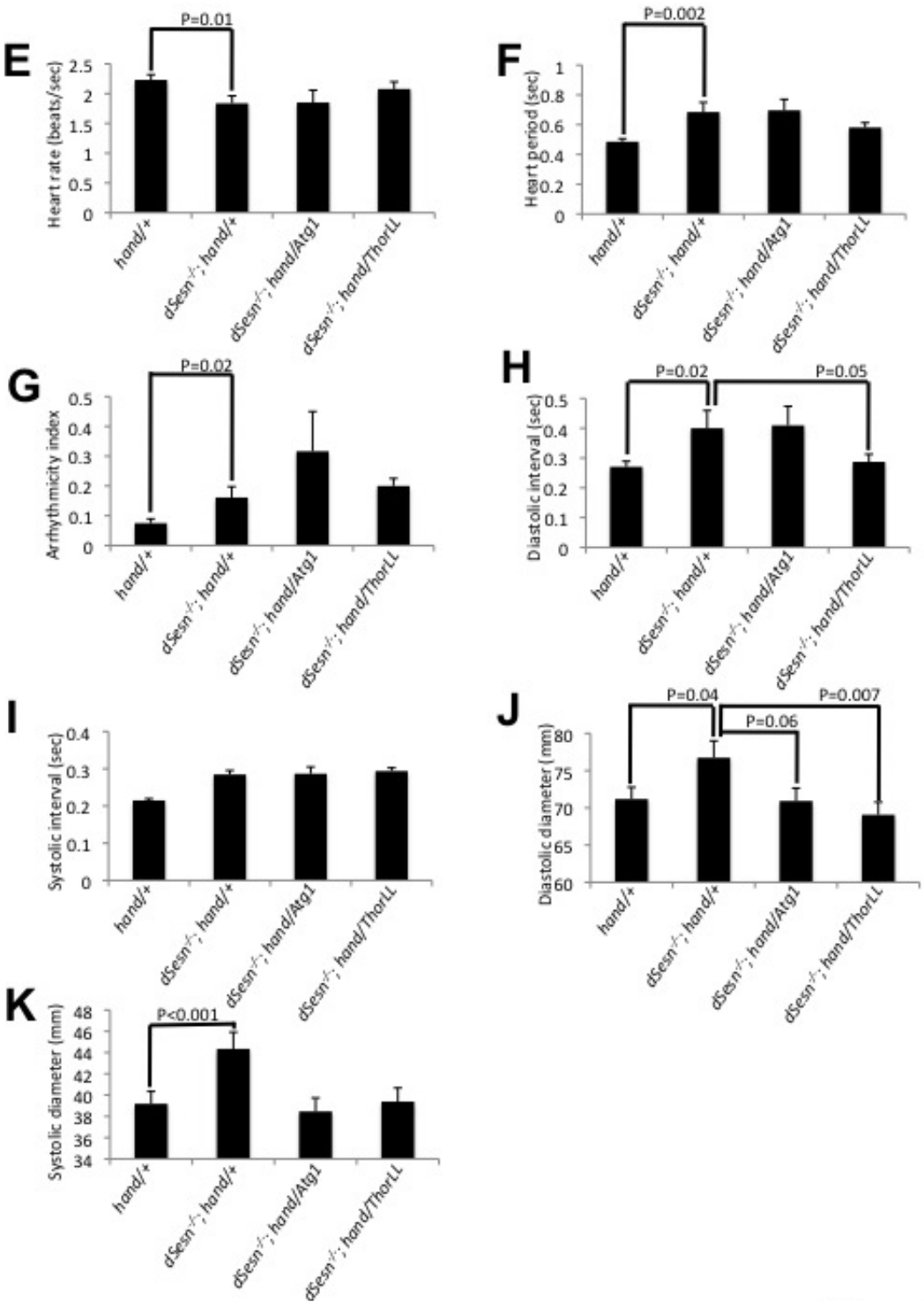

Figure 5: Continued.

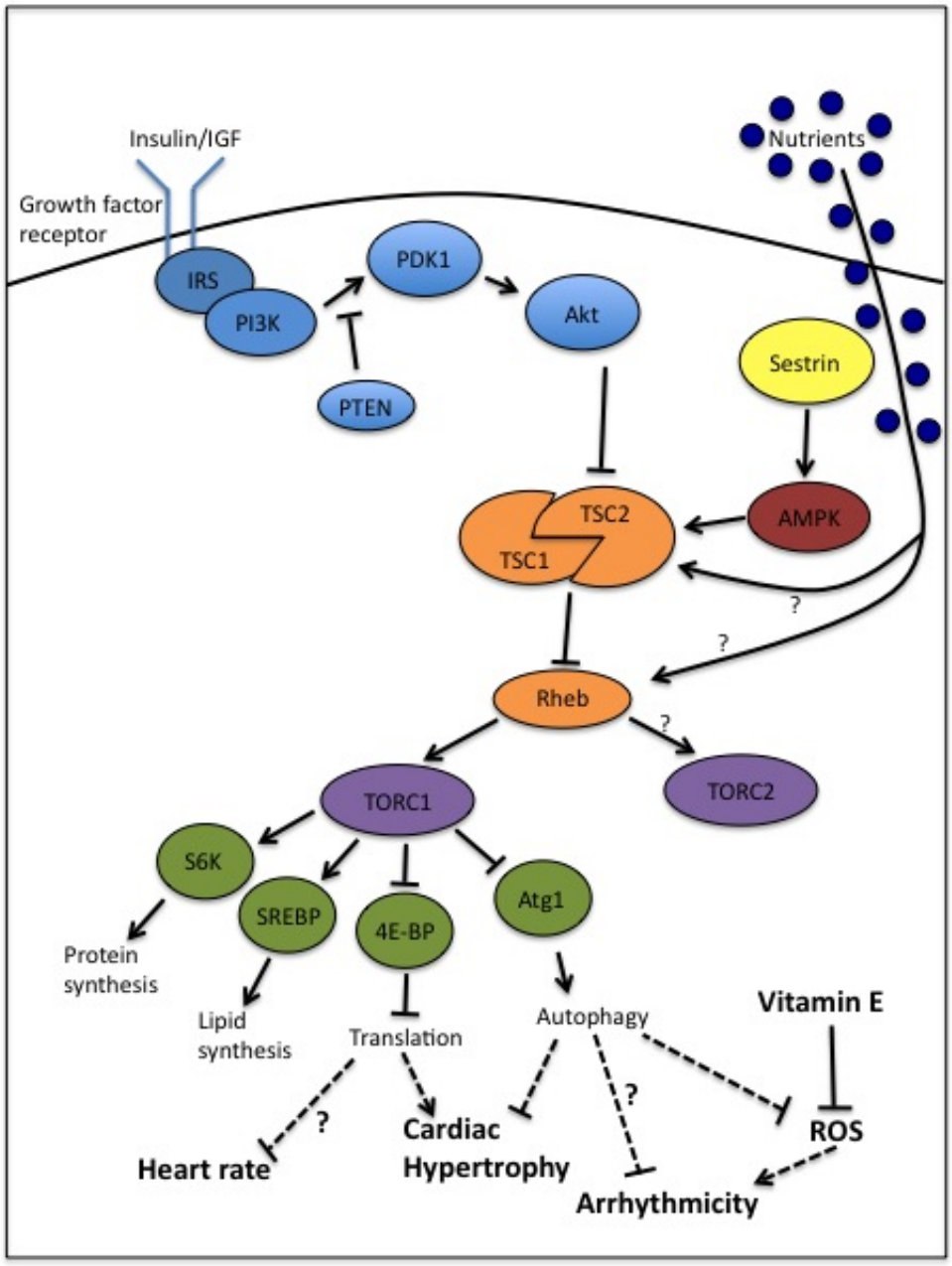

Figure 6: Model for cardiac performance regulation through TOR signaling cascade. Proposed model constructed through experimental results using cell growth regulatory element, 4E-BP, and autophagy regulatory element, Atg1, downstream of TOR kinase. Reduced translation by using a constitutively active form of 4E-BP results in increased heart rate and reduced diastolic diameter. Increased autophagy by overexpression of *Atg1* did not rescue arrhythmicity, however, resulted in reduced diastolic diameter.

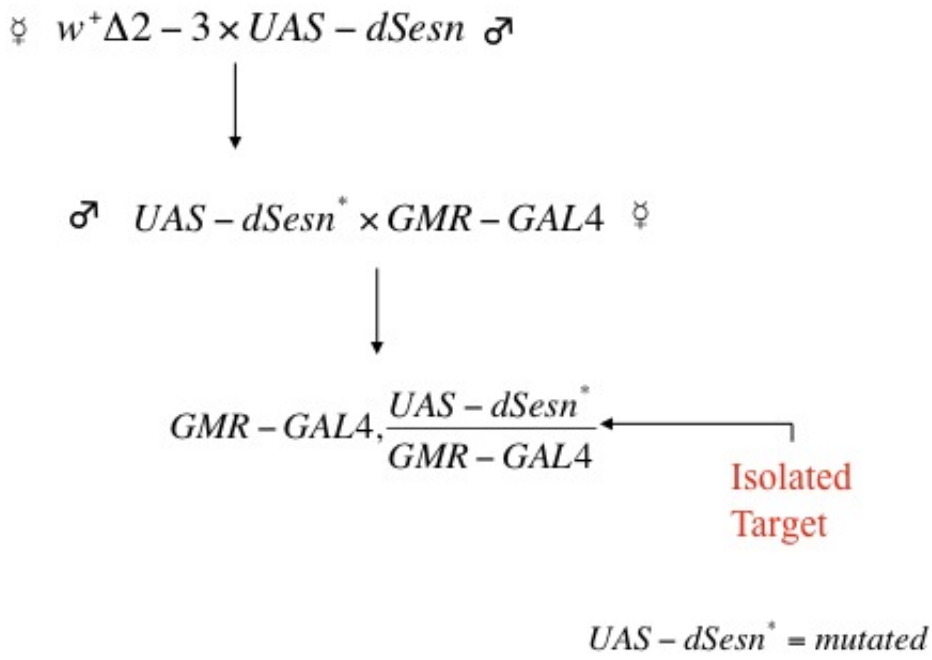

Figure 7: Genetic schemes for *UAS-dSesn* mutant isolation. Wild type *UAS-dSesn* flies were crossed with *Δ2-3 transposase* flies to generate mutant *UAS-dSesn** flies. These progenies were then crossed with eye specific driver, *gmr-GAL4*, to generate *UAS-dSesn*/gmr-GAL4* flies. Approximately 50,000 target organisms were screened.

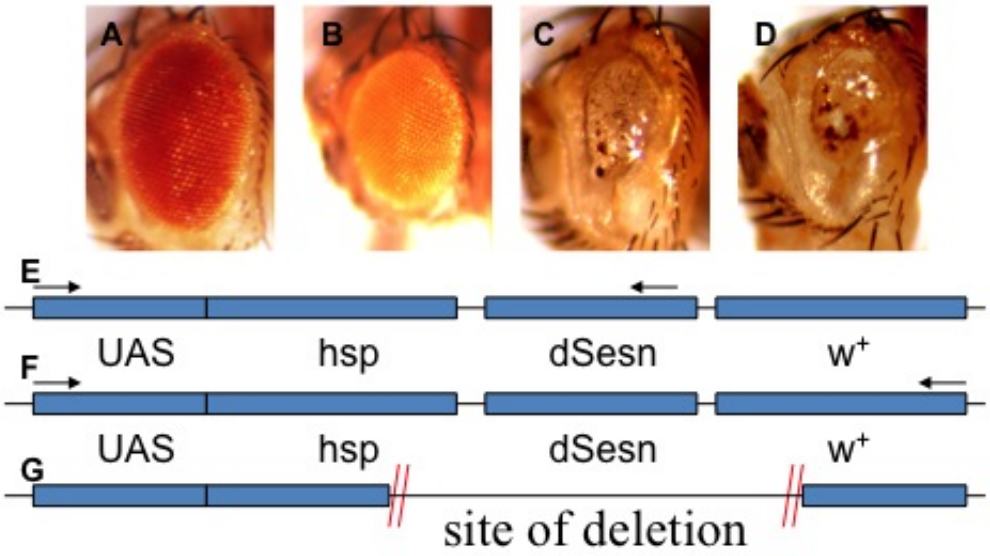

Figure 8: Phenotypes and molecular analysis of NEF allele. (A) *UAS-dSesn/GMR-GAL4* eye is shown to have a slightly overgrowth phenotype compared to wild type eyes. (B and C) *UAS-NEF* without the *GAL4* driver is shown to have normal eye morphology while *UAS-NEF/GMR-GAL4* progenies show dramatically disfigured eye morphology with hindered growth. Isolation of *UAS-NEF, GMR-GAL4/CyO* through recombination also yielded an identical phenotype as *UAS-NEF/GMR-GAL4* mutants. (E and F) Primers were designed flanking the vector insertion site of *dSesn*. (G) Only E produced successful PCR results and was shown to have a total deletion of the *dSesn* insertion.

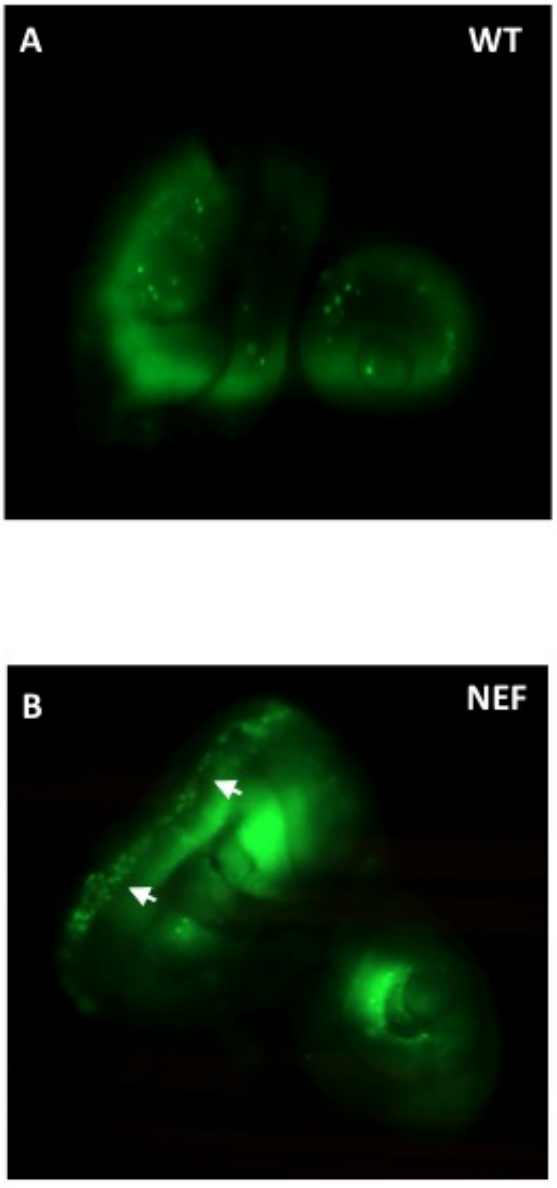

Figure 9: Acridine-Orange staining to detect cell death. The eye disk was dissected and stained using acridine-orange to detect cell death. Enhanced cell death is observed when *UAS-NEF* is expressed in the eye using *gmr-GAL4* driver as indicated by the arrows in panel B. This suggests that the *NEF* phenotype may be due to a different gene expression since *Sestrin* overexpression is not known to cause cell death.

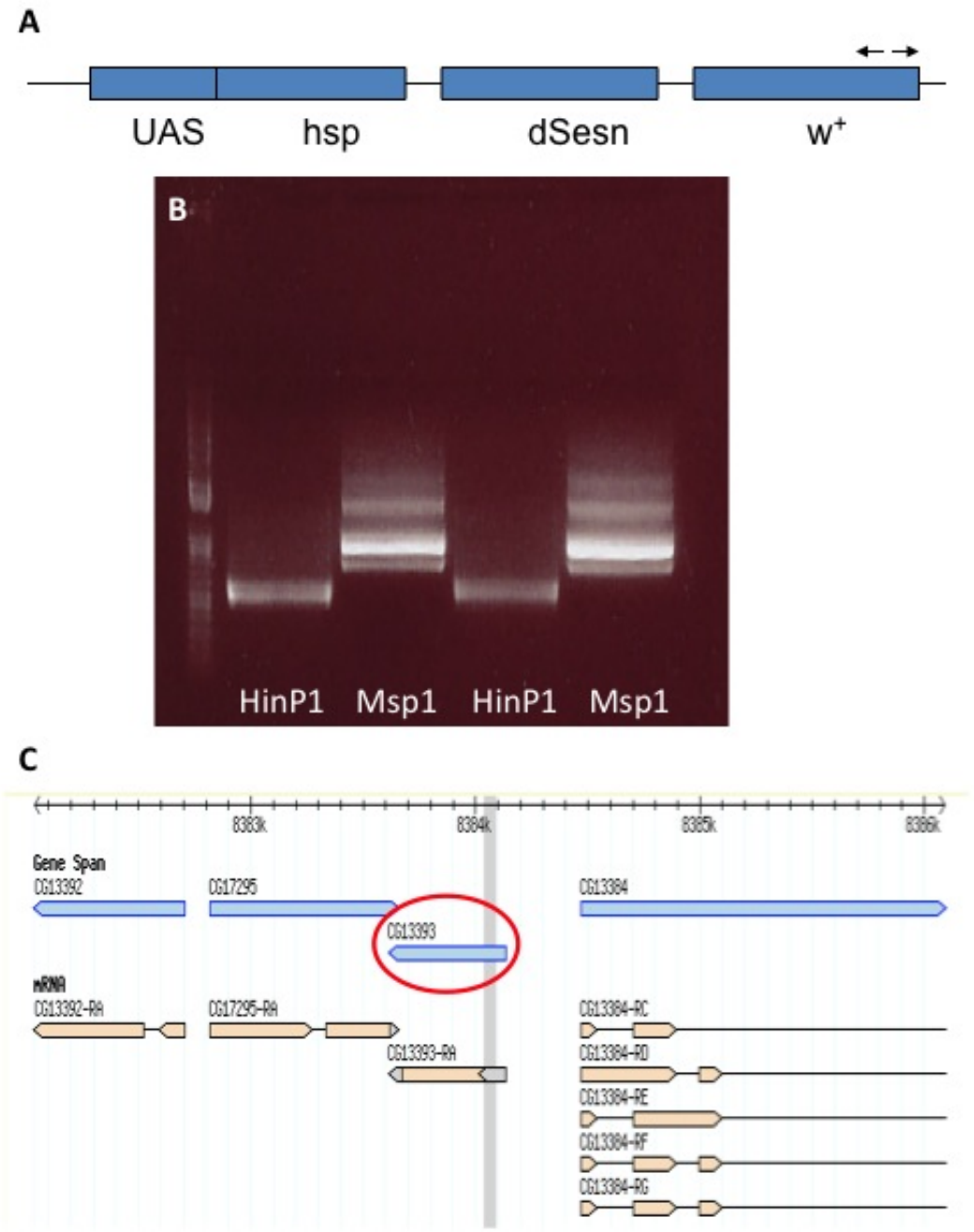

Figure 10: Inverse-PCR analysis to determine downstream gene identity. (A) Inverse PCR analysis performed using primers designed at the end of the w^+ regions. This region was selected because previous analysis showed that the end of the w^+ region was still intact in the mutant. (B) Gel picture of theh inverse PCR results for each restriction enzyme used. (C) Sequenced inverse PCR band indicates that the gene responsible for NEF phenotype may be *CG13393*, or *Dad-1* as indicated by the circle in panel C.

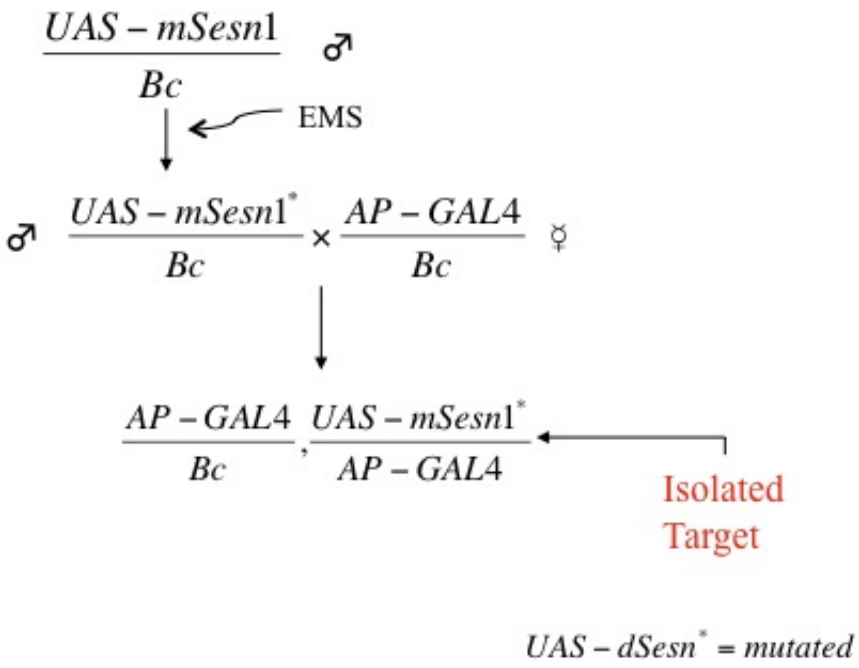

Figure 11: Genetic schemes for EMS mediated mutagenesis of *mSesn1*. *UAS-mSesn1/Bc* males were collected and subject to EMS mutagenesis overnight. These males were then crossed to wing specific driver, *ap-GAL4/Bc*, virgins to generate *UAS-mSesn1*/ap-GAL4* progenies. Approximately 35,000 target organisms were screened.

Reference

Bokel C. (2008) EMS Screens. *Methods in Molecular Biology*. 420, 119-138

Budanov A. V., Shoshani T., Faerman A., Zelin E., Kamer I., Kalinski H., Gorodin S., Fishman A., Chajut A., Einat P., Skaliter R., Gudkov A. V., Chumakov P. M., and Feinstein E. (2002) Identification of a novel stress-responsive gene Hi95 invovled in regulation of cell viability. *Oncogene*. 21, 6017-6031

Budanov A. V., Sablina A. A., Feinstein E., Koonin E. V., and Chumakov P. M. (2004) Regeneration of peroxiredoxins by p53-regulated sestrins, homologs of bacterial AhpD. *Science*. 304, 596-600

Budanov A. V., and Karin M. (2008) p53 target genes Sestrin1 and Sestrin2 connect genotoxic stress and mTOR signaling. *Cell*. 134, 451-460

Chan E. Y. (2009) mTORC1 phosphorylates the ULK1-mAtg13-FIP200 autophagy regulatory complex. *Science Signaling*. 2, 51-53

Dobrosotskaya I. Y., Seegmiller A. C., Brown M. S., Goldstein J. L. and Rawson R. B. (2002) Regulation of SREBP processing and membrane lipid production by phospholipids in Drosophila. *Science*. 296, 879-883

Grewal S. S. (2009) Insulin/TOR signaling in growth and homeostasis: A view from the fly world. *International Journal of Biochemistry and Cell Biology*. 41, 1006-1010

Grönke S., Müller G., Hirsch J., Fellert S., and Andreou A. (2007) Dual Lipolytic Control of Body Fat Storage and Mobilization in *Drosophila*. *PLoS Biol* 5(6): e137. doi:10.1371/journal.pbio.0050137

Guichard A., Srinivasan S., Zimm G., and Bier E. (2002) A screen for dominant mutations applied to components in the Drosophila EGF-R pathway. *PNAS*. 99, 3752-3757

Hara T., Nakamura K., Matsui M., Yamamoto A., Nakahara Y., Suzuki-Migishima R., Yokoyama M., Mishima K., Saito I., Okano H., and Mizushima N. (2006) Suppression of basal autophagy in neural cells causes neurodegenerative disease in mice. *Nature*. 441, 885-889

Harrison D. E., Strong R., Sharp Z. D., Nelson J. F., Astle C. M., Flurkey K., Nadon N. L., Wilkinson J. E., Frenkel K., Carter C. S., Pahor M., Javors M. A., Fernandez E., and Miller R. A. (2009) Rapamycin fed late in life extends life span in genetically heterogeneous mice. *Nature*. 460, 392-395

Hay N., and Sonenberg N. (2004) Upstream and downstream of mTOR. *Genes and Development*. 18, 1926-1945

Kundu M., and Thompson C. B. (2007) Autophagy: basic principles and relevance to disease. *Annual review of pathology: mechanisms of disease*. 3, 427-455

Laplante M., and Sabatini D. M. (2009) An emerging role of mTOR in lipid biosynthesis. *Current biology*. 19, R1046-R1052

Lee J. H., Budanov A. V., Park E. J., Birse R., Kim T. E., Perkins G. A., Ocorr K., Ellisman M. H., Bodmer R., Bier E., and Karin M. (2010) Sestrin as a feedback inhibitor of TOR that prevents age-related pathologies. *Science*. 327, 1223-1228

Levine B., and Kroemer G. (2008) Autophagy in the pathogenesis of disease. *Cell*. 132, 27-42

Martin D. E., and Hall M. N. (2005) The expanding TOR signaling network. *Current Opinion in Cell Biology*. 17, 158-166

McPhee C. K., and Baehrecke E. H. (2009) Autophagy in Drosophila melanogaster. *Biochimica et Biophysica Acta*. doi:10.1016/j.bbamcr.2009.02.009

Mizushima N. (2007) Autophagy: process and function. *Genes and Development*. 21, 2861-2873

Nakai A., Yamaguchi O., Takeda T., Higuchi Y., Hikoso S., Taniike M., Omiya S., Mizote I., Matsumura Y., Asahi M., Nishida K., Hori M., Mizushima N., and Otsu K. (2007) The role of autophagy in cardiomyocytes in the basal state and in response to hemodynamic stress. *Nature Medicine*. 13, 619-624

Ocorr K.A., Crawley T., Gibson G., and Bodmer R. (2007) Genetic Variation for Cardiac Dysfunction in *Drosophila*. PLoS ONE 2(7): e601. doi:10.1371/journal.pone. 0000601

Oldham S., and Hafen E. (2002) Insulin/IGF and target of rapamycin signaling: a TOR de force in growth control. *Trends in Cell Biology*. 13, 79-85

Pan T., Kondo S., Le W., and Jankovic J. (2008) The role of autophagy-lysosome pathway in neurodegeneration associated with Parkinson's disease. *Brain*. doi:10.1093/brain/awm318

Poireier P., Giles T. D., Bray G. A., Hong Y., Stern J. S., Pi-Sunyer F. X., and Eckel R. H. (2006) Obesity and Cardiovascular Disease: Pathophysiology, Evaluation, and Effect of Weight Loss. *Circulation*. 113, 898-918

Porstmann T., Santos C. R., Griffiths B., Cully M., Wu M., Leevers S., Griffiths J. R., Chung Y., and Schulze A. (2008) SREBP activity is regulated by mTORC1 and contributes to Akt-dependent cell growth. *Cell metabolism*. 8, 224-236

Towler M C., and Hardie D. G. (2007) AMP-activated protein kinase in metabolic control and insulin signaling. *Circulation Research*. 100, 328-341

Velasco-Miguel S., Buckbinder L., Jean P., Gelbert L., Talbott R., Laidlaw J., Seizinger B., and Kley N. (1999) PA26, a novel target of the p53 tumor suppressor and member of the GADD family of DNA damage and growth arrest inducible genes. *Oncogene*. 18, 127-137

Wang T., Lao U. and Edgar B. A. (2009) TOR-mediated autophagy regulates cell death in Drosophila neurodegenerative disease. *Journal of Cell Biology*. 186, 703-711

Wessels R., Fitzgerald E., Piazza N., Ocorr K., Morley S., Davies C., Lim H. Y., Elmen L., Hayes M., Oldham S., and Bodmer R. (2009) *d4eBP* acts downstream of both dTOR and dFoxo to modulate cardiac functional agining in *Drosophila*

Wullscheleger S., Loewith R. and Hall M. N. (2004) TOR Signaling in growth and metabolism. *Cell*. 124, 471-484